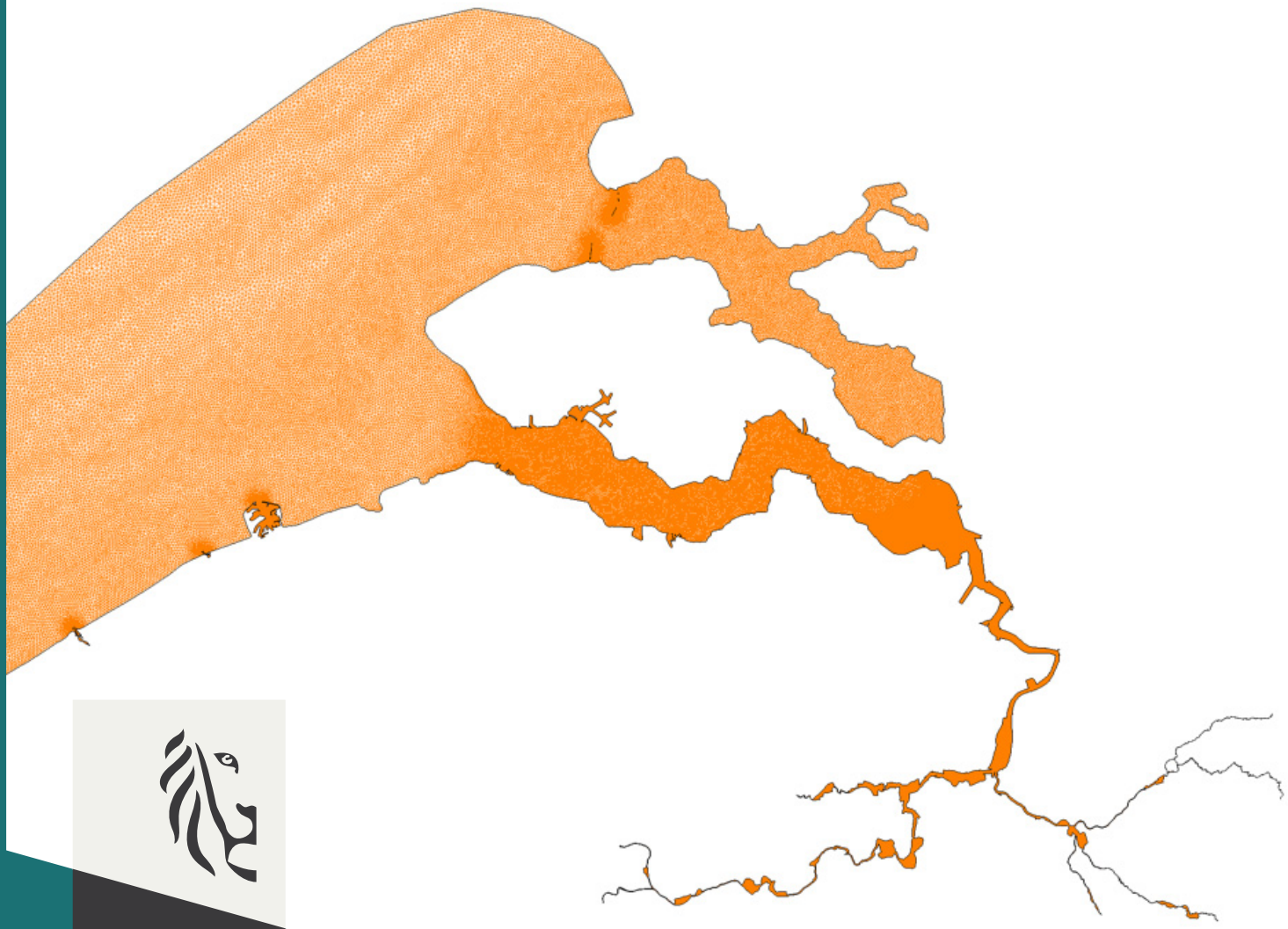

Flanders
State of
the Art

13_131_10
FHR reports

Integraal Plan Boven-Zeeschelde

Deelrapport 10
Scaldis Sand: a sand transport model for the Scheldt estuary

DEPARTMENT
**MOBILITY &
PUBLIC
WORKS**

www.flandershydraulicsresearch.be

Integraal Plan Boven-Zeeschelde

Sub report 10 –
Scaldis Sand: a sand transport model for the Scheldt estuary

Smolders, S.; De Maerschalck, B.; Plancke, Y.; Vanlede, J.; Mostaert, F.

Flanders Hydraulics Research
Flanders State of the Art

Cover figure © The Government of Flanders, Department of Mobility and Public Works, Flanders Hydraulics Research

Legal notice

Copyright and citation

This publication should be cited as follows:

Smolders, S.; De Maerschalck, B.; Plancke, Y.; Vanlede, J.; Mostaert, F. (2019). Integraal Plan Boven-Zeeschelde: Sub report 10 – Scaldis Sand: a sand transport model for the Scheldt estuary. Version 2.0. FHR Reports, 13_131_10. Flanders Hydraulics Research: Antwerp.

Document identification

Customer:	Flanders Hydraulic Research	Ref.:	WL2019R13_131_10
Keywords (3-5):	Scaldis, TELEMAC, SISYPHE, sand transport model		
Text (p.):	45	Appendices (p.):	8
Confidentiality:	☒ No	☒ Available online	

Author(s)	Sven Smolders

Control

	Name	Signature
Reviser:	Bart De Maerschalck Yves Plancke	Getekend door: Bart De Maerschalck (Signa Getekend op: 2019-10-14 10:34:02 +01:00 Reden: Ik keur dit document goed Bart De Maerschalck Getekend door: Yves Plancke (Signature) Getekend op: 2019-10-22 15:58:56 +01:00 Reden: Ik keur dit document goed Yves Plancke
Project leader:	Joris Vanlede	Getekend door: Joris Vanlede (Signature) Getekend op: 2019-10-22 17:01:45 +01:00 Reden: Ik keur dit document goed Joris Vanlede
Approval		
Head of Division:	Frank Mostaert	Getekend door: Frank Mostaert (Signature) Getekend op: 2019-10-14 11:25:04 +01:00 Reden: Ik keur dit document goed Frank Mostaert

Samenvatting

De Vlaamse Waterweg NV wil de bevaarbaarheid van de Boven-Zeeschelde verbeteren zodat schepen tot klasse Va er kunnen passeren. Hiervoor werd een integraal plan Boven-Zeeschelde opgesteld dat de conclusies van een haalbaarheidsstudie, eerder uitgevoerd, verder zou toetsen. Het is van cruciaal belang dat de aanpassingen aan de Boven-Zeeschelde om de bevaarbaarheid te verhogen, eveneens leiden tot het minstens behouden van en graag verbeteren van de veiligheid tegen overstromingen en het behoud van het natuurlijk ecosysteem.

Dit rapport beschrijft de opbouw van een zandtransportmodel voor het Schelde-estuarium, waarbij de nadruk ligt op de Zeeschelde, meer bepaald op de Boven Zeeschelde. Binnen het project Integraal Plan Boven-Zeeschelde is het belangrijk om de effecten van veranderingen in de Boven-Zeeschelde juist in te schatten. Dit zandtransportmodel vormt een op zichzelf staand onderdeel binnen een hele modellentrein om verschillende scenario's te toetsen.

Het zandtransportmodel hier beschreven bouwt verder op ervaringen opgedaan in andere projecten binnen en buiten het Waterbouwkundig Laboratorium. De vergaarde kennis is beschreven in een literatuurstudie. Vanuit die voorgaande ervaringen werd er gekozen om een zandtransportmodel te maken met één fractie zand, die een D50 waarde heeft van 150 µm. Het zand wordt uniform over de bodem van heel het estuarium verdeeld. Er werd gekozen om de Engelund en Hansen transportvergelijking te gebruiken. Het zandtransportmodel werd gekoppeld aan een bestaand TELEMAC-3D hydrodynamisch model, Scaldis, dat eerder binnen het kader van dit project al ontwikkeld werd. Alhoewel de modelsoftware in staat is de veranderingen van de bodem ten gevolge van de sedimentatie en erosie te berekenen, is er binnen dit project voor gekozen om voor de hydrodynamische berekening de bodem in het model constant te houden gedurende de duur van de simulatie. Er is in het model dus geen feedback van een veranderende bodem op de stroming en waterstanden. De sedimentatie en erosie van de bodem worden wel in het sedimenttransportmodel (SISYPHE) bijgehouden en kunnen als variabele opgevraagd worden.

De modelresultaten worden getoetst aan puntmetingen van sedimenttransport uit een voor dit project speciaal uitgevoerde meetcampagne. Het model was in staat om het zandtransport voor de meeste locaties zeer goed te simuleren (bv. Oosterweel en Dendermonde), zowel wat de grootteorde betreft alsook de eb- en vloedpieken in transport. Enkele locaties gaven minder goede resultaten, maar daar waren de eb- en vloedpiek in de metingen ook niet goed te onderscheiden (bv. Driegoten).

Verder werd het zandtransport over verschillende dwarssecties van het estuarium berekend en vergeleken met een eerder opgemaakte zandbalans voor de Zeeschelde. Deze zandbalans werd berekend op basis van het verschil in bathymetrie van 2001 en 2010 en lithologische informatie. Het zandtransport van het model tijdens een springtij-doodtij cyclus werd geëxtrapoleerd naar het transport gedurende een jaar en vergeleken met de zandbalans. Voor de Boven-Zeeschelde gaf dit gelijkaardige resultaten en ook de richting van het transport was bij beide gevallen stroomafwaarts. Voor de Beneden-Zeeschelde gaf het model veel lagere warden (grootteorde 10 keer lager) en bovendien was het transport in het model afwaarts gericht, daar waar deze in de zandbalans opwaarts is gericht.

Tenslotte werd het zandtransport over verschillende dwarssecties langsheen heel het Schelde-estuarium gelinkt aan de getij-asymmetrie van de dwarssectie-gemiddelde stroomsnelheden tot de vijfde macht (zoals ze in de Engelund en Hansen vergelijking gebruikt worden).

Abstract

De Vlaamse Waterweg NV (DVW) wants to improve the navigability of the Upper Sea Scheldt allowing navigability up to Class Va while increasing safety for ships of class IV and lower. An integrated plan was made that aims at further developing the conclusions from a feasibility study towards Class Va shipping. It is of the utmost importance that the design of this enlargement leads to a multifunctional Scheldt with assets for navigability, guarantees for protection against flooding and a sustainable natural system.

This report present a sand model for the Scheldt estuary, that is part of a model chain to evaluate different geometrical scenarios. The behaviour of non-cohesive sediments is important in the assessment of the impact of changes in bathymetry or management of the estuary and for this project, the Upper Sea Scheldt in particular.

The sand model is coupled with a TELEMAC-3D model Scaldis, developed earlier in the project. The sand model itself uses a single fraction of sand with a D50 value of 150 µm. The Engelund and Hansen equation was chosen as total load transport equation. The bottom of the hydrodynamic model was not updated with bed level changes from the sand model.

Model results show good agreement with point measurements for some locations (Oosterweel and Dendermonde) and less agreement with other locations (Driegoten and Schoonaarde). Sand transport over different transects along the Scheldt estuary was calculated and compared with calculated transport rates based on bathymetric surveys between 2001 and 2010 and on lithological information. For the Upper Sea Scheldt the model reproduces the calculated results very well. The model underestimates sand transport in the Lower Sea Scheldt compared to the calculated transports and gives opposite directions of transport.

Finally an overview of net sand transport over different transects along the Scheldt estuary is given and linked to the tidal asymmetry of the cross-sectionally averaged flow velocity to the power five (as used in the Engelund Hansen formula).

Contents

List of tables

List of figures

1 Introduction

1.1 Integrated Plan Upper Sea Scheldt

The implementation of the Seine-Scheldt connection will result in increased shipping traffic between France and Flanders. De Vlaamse Waterweg NV (DVW) wants to improve the navigability of the Upper Sea Scheldt in order to prevent a bottle neck effect on the Canal Ghent – Terneuzen and the Western Scheldt. Additionally, an improved navigability of the Upper Sea Scheldt would also promote the shipping between the Scheldt basin and the Albert Canal (towards the river Meuse). Within this framework, an integrated plan is being developed, in which navigability, safety and nature are the key elements.

At the moment, the upstream part of the Upper Sea Scheldt is a Class IV fairway (ships up to 85m long and 9.5m wide) and forms a bottleneck in the European network. The questions that are to be answered within the integrated plan pertain to the measures that need to be taken to upgrade the Upper Sea Scheldt to a Class Va fairway suitable for ships up to 2250 tons (ships up to 110 m long and 11.4 m wide and 3.5 m draught), taking into account the other functions (safety, nature and recreation).

The outcome of a feasibility study was that with relatively small measures a balance between cost and benefit can be found, but allowing navigability up to Class Va while increasing safety for ships of class IV and lower.

The integrated plan aims at further developing the conclusions from the feasibility study towards Class Va shipping. It is of the utmost importance that the design of this enlargement leads to a multifunctional Scheldt with assets for navigability, guarantees for protection against flooding and a sustainable natural system.

The sand model presented in this report is part of a model chain to evaluate the different geometrical scenarios. The behaviour of non-cohesive sediments is important in the assessment of the impact of changes in bathymetry or management of the estuary and for this project, the Upper Sea Scheldt in particular.

1.2 Goal for the sand transport model

The goal of the sand transport model within this project is to estimate the effect of different possible measures in the Upper Sea Scheldt on non-cohesive sediment behaviour in the estuary.

The model translates geometrical changes in the Upper Sea Scheldt into the appropriate sand transport response. These different responses to different geometrical scenarios are caused by a changed hydrodynamic regime and will be explained by changes in hydrodynamic parameters like changes in ebb or flood flow velocities.

The results of the reference sand transport model (i.e. the sand transport model on top of the calibrated 2013 Scaldis 3D HD model) will be compared with point measurements of sand transport specifically executed for this goal (Plancke et al., 2014). Cross sectional averaged sand transport and transport directions will be compared with a sediment balance of the Sea Scheldt based on lithological information and bathymetry changes between 2001 and 2010 (Vandenbruwaene et al., 2017).

2 Literature review

This literature review will focus on work that has been done on modelling sand transport with a preference on modelling with TELEMAC. Most importance will be given to work done at Flanders Hydraulics Research. Other articles are discussed more briefly. At the end of this literature review a short conclusion will be written with the lessons learnt from previous work. This will form a starting point for the sand transport model described in this report.

2.1 Sensitivity analysis from WL project 15_068: Modelling the Belgian coastal zone and estuary mouth

In project 15_068: Modelling the Belgian coastal zone and estuary mouth, a 2D hydrodynamic TELEMAC model of the Belgian coastal zone extended to the Scheldt estuary (with the same contour as the Scaldis model) will be coupled with the TOMAWAC module to include wave effects and with the SISYPHE module to include sediment transport. In sub report 6 Kolokythas et al. (2018) describe three test cases of TELEMAC-2D coupled with SISYPHE.

2.1.1 Gaussian hump

In the first test case: uniform flow over a Gaussian hump, the bed is deformable and under the flow conditions the hump is expected to migrate along the direction of the flow. For this test case an approximation to an analytical solution, given by Schramkowski et al. (2016), has been used to validate the model results in terms of the migration of the hump. The main purpose of this test case in their project was to determine the migration speed of the Gaussian hump bed under different sediment transport models (for bed load) and define software limitations. And thus different software parameters were tested and their conclusions are summarized here:

- The test case was solved for different grid resolutions: 10 m, 20 m and 40 m. The grid resolution had no influence on the general solution of the test case. Only small differences were found between the different grid resolutions.
- Different widths and lengths of the channel were tested and no effect on the test case solution was found. The geometry of the domain had no significant effect on the solution.
- Different turbulence models were tested: constant viscosity, Smagorinski and k-epsilon. No difference was found in the simulation results between these three turbulence models.
- Different advection schemes were tested: method of characteristics (default, and unconditionally stable), Centered semi implicit scheme + SUPG, Upwind explicit finite volume scheme and PSI distributive scheme (mass conservative). All tested advection schemes resulted in a hump propagation with the same speed, however, the upwind explicit finite volume and the PSI distributive scheme showed spatial instabilities along the channel's width. These instabilities were the result of a cold start of the test case. Once a hot start simulation was done, these instabilities disappeared for both advection schemes.
- Three different sediment transport equations were tested: Engelund and Hansen (1967, total transport), Engelund and Hansen modified by Chollet and Cunge (1979, total transport) and Van Rijn (1984, bed load only). The latter two resulted in an insignificant movement of the hump crest over a simulated period of 62 days.
- By using the Koch and Flokstra (1981) formula, a bed slope effect was tested for different values of the beta coefficient used in the formula. If the beta coefficient is zero, no slope effect is taken into account. the larger the beta coefficient the larger the slope effect acts on the simulation results. In

fact it acts like adding a diffusion term in the bed evolution equation. This tends to smooth the results and is often used to reduce instabilities. Beta coefficients of 1.3 (default), 2.5, 5.0 and 10.0 were tested. Figure 1 shows clearly the smoothing effect of a larger beta coefficient on the results of this hump test case. The larger the beta coefficient the more the results are smoothed. The default value of beta (=1.3) is not resulting in any significant differences compared to the results without considering slope effects (beta = 0).

Figure 1 – Middle-width sections of bed level in different time instances (coarse long grid) for different beta parameter of Koch and Flokstra (1981)formula for the propagation of a Gaussian hump.

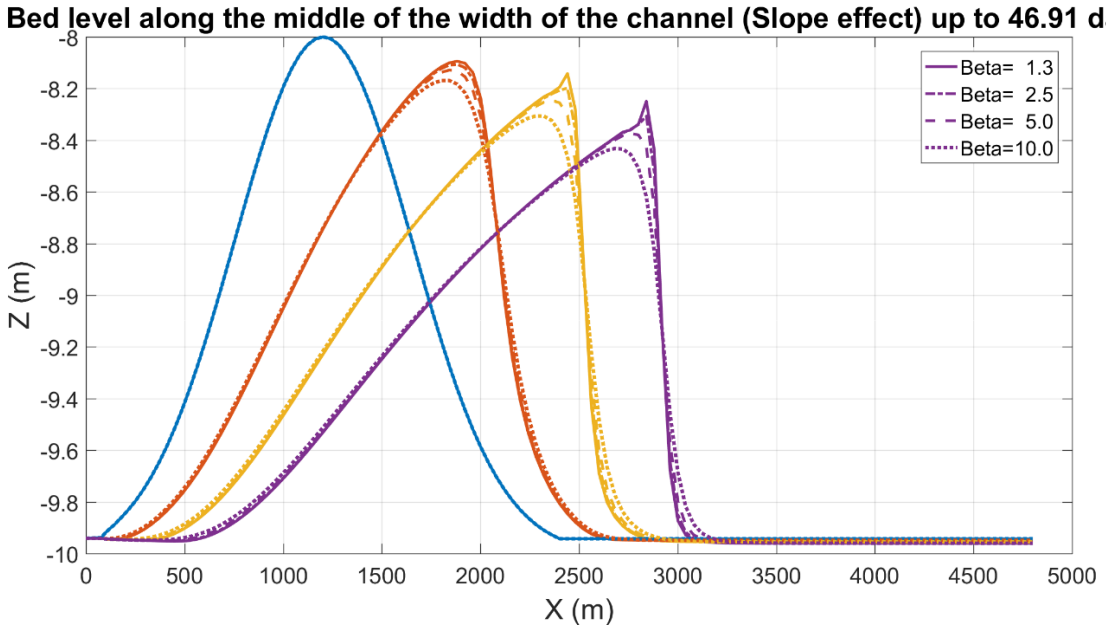

- The test case was also ran with different morphological factors: 1, 10 and 100. This factor is used to speed up the morphological process. The morphological factors 1 and 10 gave similar results, but the morphological factor 100 resulted in a temporal hysteresis in the propagation of the hump, i.e. it slowed down the propagation of the hump. These values could have different effects on different type of cases!
- When activating suspended sediment it appears that more sediment is gathered near the lateral boundaries than in the middle of the channel. This problem is solved by using advection scheme 15 and deactivating the diffusion terms.
- the test case was also run in TELEMAC-3D, using 20 vertical layers and a horizontal turbulence model of Smagorinski and for the vertical turbulence model the mixing length model by Nezu and Nagakawa (the turbulence models are the same as used in the 3D Scaldis model). The 3D solution included wiggles on the hump's crest as the hump propagates. A finer vertical resolution close to the solid bed was used in order to try to solve this problem, but without any success. Different default values for the SUPG option are related to this problem, but no further test were done, trying to improve the results.

2.1.2 Channel trench

The second test case consists of the same channel but instead of a hump a trench is modelled. All numerical parameters were kept identical to the first test case of the hump for better comparison possibilities. Not so many parameters were tested as in the previous test case, but the results and conclusions are again briefly summarized here:

- To test the influence of the value of the beta coefficient of the slope effect (Koch and Flokstra, 1981), different values were tested: 0, 1.3 (default if slope effect is activated), 2.5 and 5.0. a beta value equal to 0 or 1.3 resulted into an unnatural instability on the back side of the trench. Higher values of the beta parameter result in faster dispersion of the trench. It seemed that a value of 2.5 for the beta coefficient solved the instability without invoking too much dispersion to the results.
- A morphological factor of 1, 10 and 100 was tested and the results were the same as for the hump test case. A factor 1 or 10 gave the same results, but with a factor of 100 the results were slightly different.
- Using suspended transport instead of bed load transport gave the same results as for the hump test case.
- Like the hump test case, this test case was also simulated in TELEMAC-3D with the same parameter settings as the 3D hump test case. The trench propagates with the same speed in 2D and 3D, but the 3D simulation shows instabilities (wiggles in the sediment) in front of the trench. These results are similar to the hump test case. These instabilities are attributed to the different upwind configuration of the advection scheme in TELEMAC-2D and 3D.

2.1.3 Tidal inlet case

In the same report of Kolokythas et al. (2018) a test case is presented where TELEMAC-2D is coupled with SISYPHE to investigate the autonomic morphological evolution of a tidal inlet (Figure 2), starting from an initially flat bottom. They investigated the performance of the coupled TELEMAC2D-SISYPHE morphodynamic model for simulating morphology at long-term time scales. In doing this various model parameters were extensively analyzed how they affected the model results. This model was based on a similar model developed in the past (Nnafie *et al.*, 2015) and it results were compared with those of earlier published studies. Specifically, the case study in Nnafie *et al.* (2015) was identical to the one reported in Ridderinkhof *et al*. (2014), in which the long-term evolution of ebb-tidal deltas that form in tidal inlet-basin systems was studied using the numerical model Delft3D. The comparison of the two numerical models showed that the hydrodynamic quantities agreed well with each other in the tidal inlet area. Differences were found close to the seaward boundaries though, due to the differences in the way of imposing the hydrodynamic boundary conditions. As for the morphodynamic comparison, results from an extensive exploration of the numerical parameters in TELEMAC-2D showed that although the model achieved to simulate an ebb-tidal delta offshore of the tidal inlet and tidal channels through this inlet, no clear branching patterns of tidal channels were formed in the tidal basin due to strong numerical diffusion. Decreasing of grid size (> 2.5 times) might improve results, but it affected substantially the computational times. The work done by Kolokythas et al. (2018) was to further investigate model parameters to improve this branching pattern at the tidal inlet. The main default TELEMAC-2D and SISYPHE model parameters are given in Table 1 and for more details about the case we refer to Kolokythas et al. (2018) and Nnafie et al. (2015). Here a summary is made with the most important findings and solutions for better parameter values to couple TELEMAC with SISYPHE.

Figure 2 – Computational domain and bathymetry for the idealized tidal inlet model (copy from Kolokythas et al., 2018).

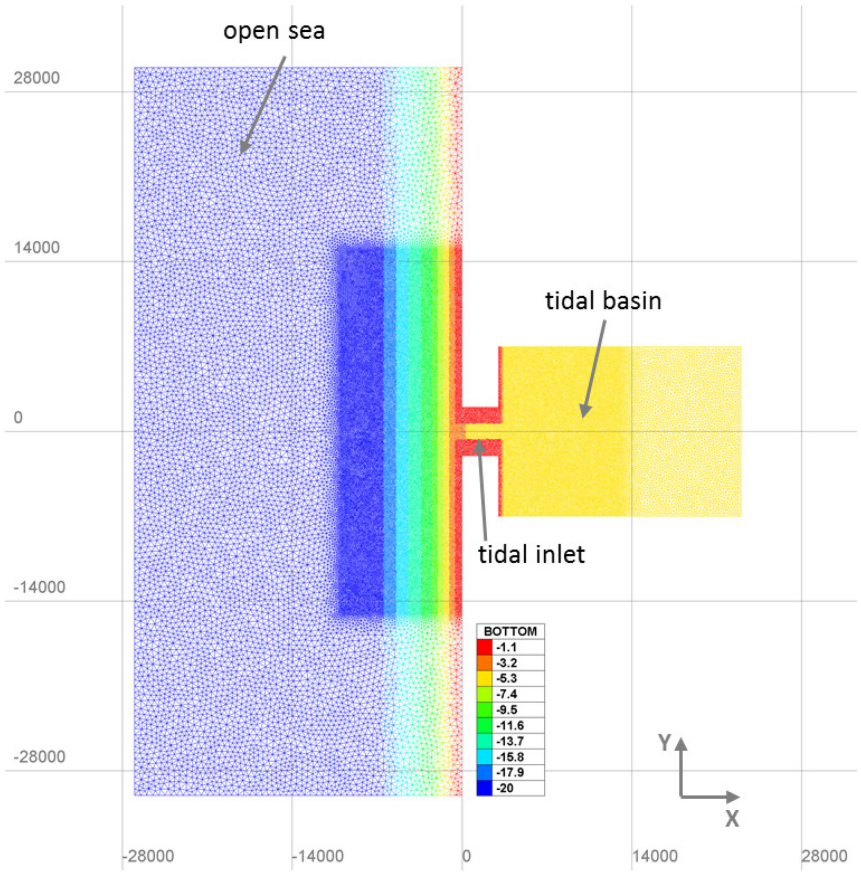

Table 1 – Main default TELEMAC-2D and SISYPHE model parameters for the case of the idealized tidal inlet runs (after Kolokythas et al., 2018).

	Parameter	**Value**
TELEMAC-2D	*EQUATIONS*	*SAINT-VENANT FE*
	TYPE OF ADVECTION	*1;5 (characteristics, PSI)*
	SUPG	*0;1*
	SOLVER	*3 (conjugate grad on normal eq.)*
	TREATMENT OF TIDAL FLATS	*1*
	OPTION FOR LIQUID BOUND	*1*
	INITIAL ELEVATION	*0*
	COUPLING PERIOD FOR SISYPHE	*1*
	CORIOLIS COEFFICIENT	*$1.43 \cdot 10^{-4}$ s^{-1}*
	CONSTANT VISCOSITY	*10^{-4} m^2/s*
	DIFFUSIVITY	*10^{-2} m^2/s*
	CHEZY	*65 $m^{1/2}/s$*
SISYPHE	*TOTAL LOAD TRANSPORT FORMULA*	*30 (Engelund & Hansen, 1967)*
	SUSPENSION	*NO*
	FORMULA FOR SLOPE EFFECT	*1 (Koch & Flokstra) Beta=1*
	FORMULA FOR DEVIATION	*1 (Koch & Flokstra)*

Software version

The results of the test case of the tidal inlet were resimulated with TELEMAC version V7P2r2 without changing any of the input parameters in the steering file and were compared with the results presented by Nnafie et al. (2015), who did his tests with TELEMAC version V6P3r1. Figure 3 shows that there are substantial differences in bed evolution at the area of the tidal inlet after a simulation period of 15 years. The main difference observed was that version V7P2r2 gave more fractal patterns in the back-barrier basin and that this version showed spikes in the solution. No clear reason or difference between both software versions was given.

Figure 3 – Bed level change [m] at the area of the tidal inlet (zoom) obtained by versions 6p3r1 (left) and 7p2r2 (right) after a simulation period of 14.7 years (copy from Kolokythas et al., 2018).

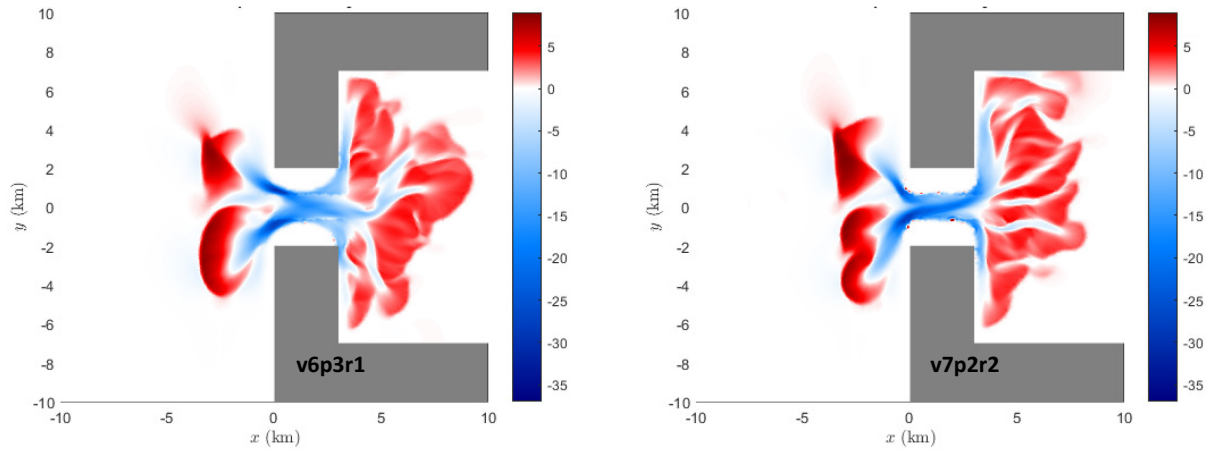

Hydrodynamic boundary conditions

On the north side of the model large velocities were found entering the domain. After extensive testing they found these high velocities were caused by the imposed Coriolis force. When they considered a Coriolis parameter of opposite sign (meaning that the tidal inlet was located in the Southern hemisphere) this resulted into the transfer of the problematic behavior to the southern boundary of the domain. Any relevant problematic behavior at the open sea boundaries was eliminated after deactivating the Coriolis force. The Coriolis force has an impact on the direction of the velocity vectors entering the domain, which are rotating during the tidal cycle, heading towards the coast at very shallow waters for a certain period of the tidal cycle. This is not trivial to compute numerically. When the Coriolis force is turned off, the velocity field close to the open sea boundaries remains always parallel to the coast, which gives no substantial problems numerically.

Morphological boundary conditions

The default settings for the open boundary in SISYPHE are an imposed bed evolution (LIEBOR=5 and LIQBOR=4) equal to zero. A simulation with different settings, i.e. with zero sediment transport rate (LIEBOR=4 and LIQBOR=5), was tested. A big influence of sediment accumulation or the absence of that was found close to the boundaries and this affected also the morphodynamics in the inlet region itself. No transport rates at the boundaries slightly enhances morphodynamics. Applying a non-erodible bed at the boundaries of the model domain further improved the sediment behaviour at the boundaries, but did not completely solved it. There is still accumulation of sediment near the boundary. Application of this non-erodible bed condition near the boundaries also affected the morphodynamics in the tidal inlet zone, even more than just switching between boundary types.

Initial conditions and spin up of the model

Changing the initial free surface in the model domain from zero to 0.686 m (this equal the amplitude of the M2 tidal component used in this model) significantly changed the morphological pattern in the back-barrier basin of this tidal inlet case after a simulation period of 15 years (Figure 4). When giving the model a spin up period of six tidal cycles before starting SISYPHE also leads to a substantially different morphological pattern in the back-barrier basin of the model (Figure 5).

Figure 4 – Bed level change [m] obtained by considering zero initial free surface elevation (left) and an initial elevation equal to 0.686 m (right) after a simulation period of 14.7 years.
The figures zoom at the area of the tidal inlet (copy from Kolokythas et al., 2018).

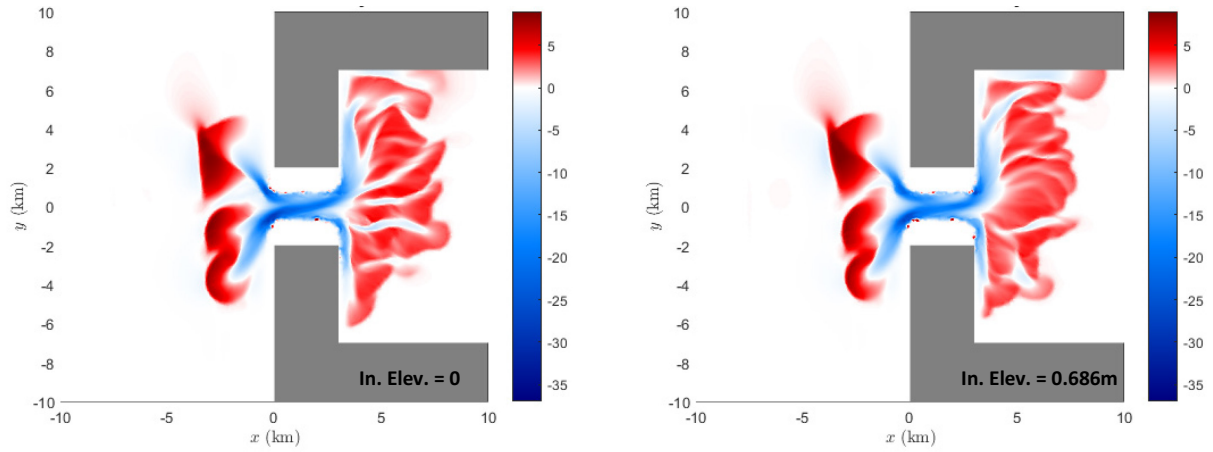

Figure 5 – Bed level change [m] obtained by considering no spin up period of the model (left) and a spin up period of 6 tidal cycles (72 h) (right) after a simulation period of 14.7 years.
The figures zoom at the area of the tidal inlet (copy from Kolokythas et al., 2018).

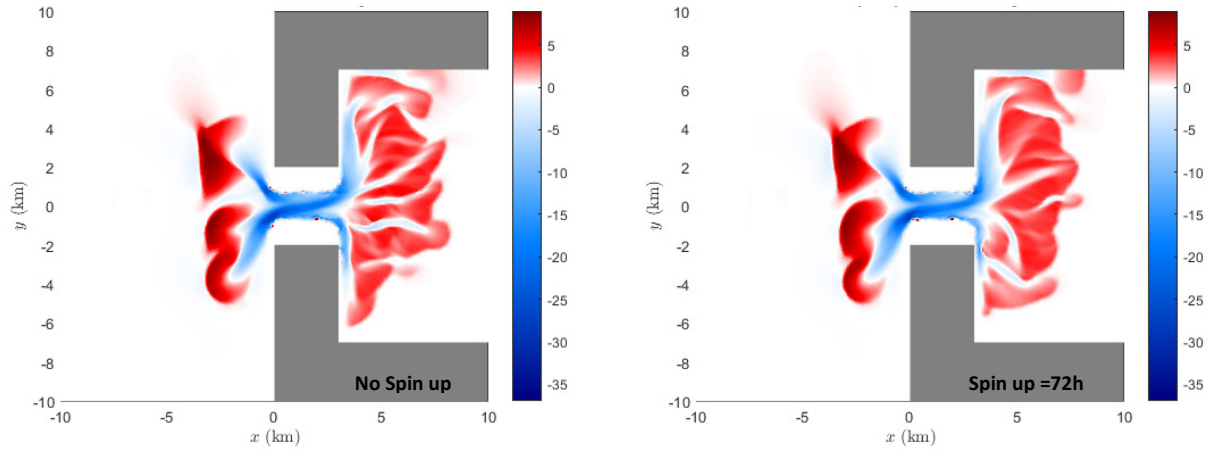

Morphological acceleration

No big differences were found applying a morphological acceleration of 10 or 1 to the model.

Sediment transport formulation

All tidal inlet simulations were simulated using the total load transport formula proposed by Engelund and Hansen (1967) (ICF = 30 in SISYPHE), while suspension of sediment was not considered. Other total load and bed load formulas were tested in order to investigate their impact on the long term evolution of the tidal inlet system. Specifically, the modified (to account for sand dunes) Engelund & Hansen total load

formula (ICF=3), the Van Rijn's bed load formula (ICF=7), and the Bijker's total load formula (ICF=4), were considered. The bed level change in the tidal inlet area after a simulation period of about 10 years for the aforementioned sediment transport formulas is presented in Figure 6. It was found that only the Engelund and Hansen (ICF = 30) total load formula leads to a bed evolution pattern comparable to the tidal inlet systems observed in the field. The rest of the formulas presented rather high diffusive behavior.

Adding suspended load transport was also tested. The default options for suspension of sediment were selected, except for the option for the reference concentration formula (gives the near bed concentration of sediment), the effect of which was tested and results are given in Figure 7. For the simulations of the total load transport, the Van Rijn's bed load formula was applied together with the advection-diffusion equation for suspended load transport. The choice of the reference concentration formula is of great importance given the difference between their results. Van Rijn's reference formula leads to more realistic results presenting a complex branching pattern in the tidal basin similar to the fractal patterns observed in the real tidal inlet systems. The advection-diffusion equation coupled with the use of a semi-empirical formula for bed load transport lead to a totally different prediction for the evolution of the tidal inlet area (see Figure 6 (a) and Figure 7 (right)).

Figure 6 – Bed level change [m] obtained by use of three different total load and one bed load transport formulas after a simulation period of 9.6 years; (a) Engelund & Hansen - 30, (b) Engelund & Hansen - 3, (c) Van Rijn – 7 (bed load only), (d) Bijker – 4. The figures zoom at the area of the tidal inlet (copy from Kolokythas et al., 2018).

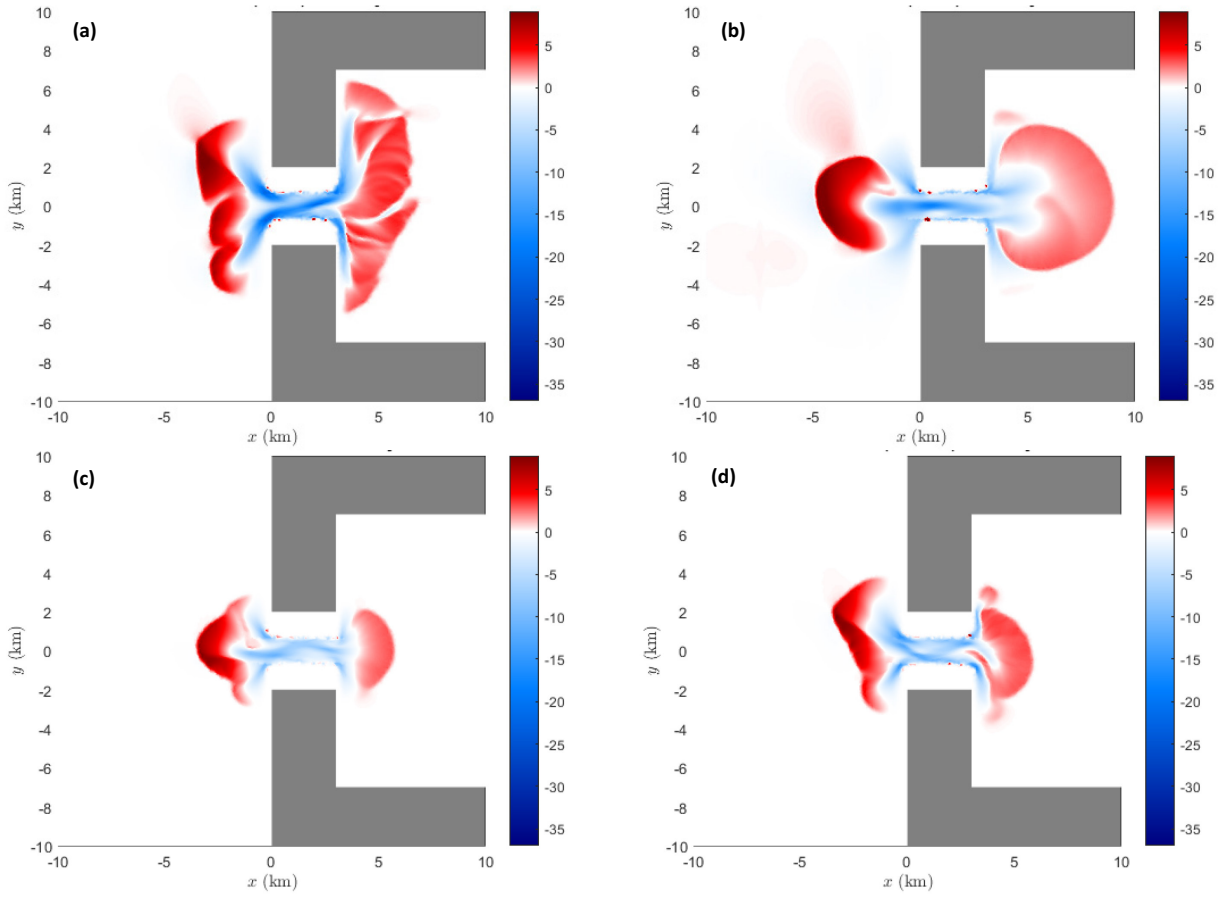

Figure 7 – Bed level change [m] obtained by considering suspended sediment transport (advection-diffusion equation) and bed load transport by Van Rijn's formula after a simulation period of 9.6 years; Reference concentration is given by Soulsby-Van Rijn's formula (left) and by Van Rijn's formula (right).
The figures zoom at the area of the tidal inlet (copy from Kolokythas et al., 2018).

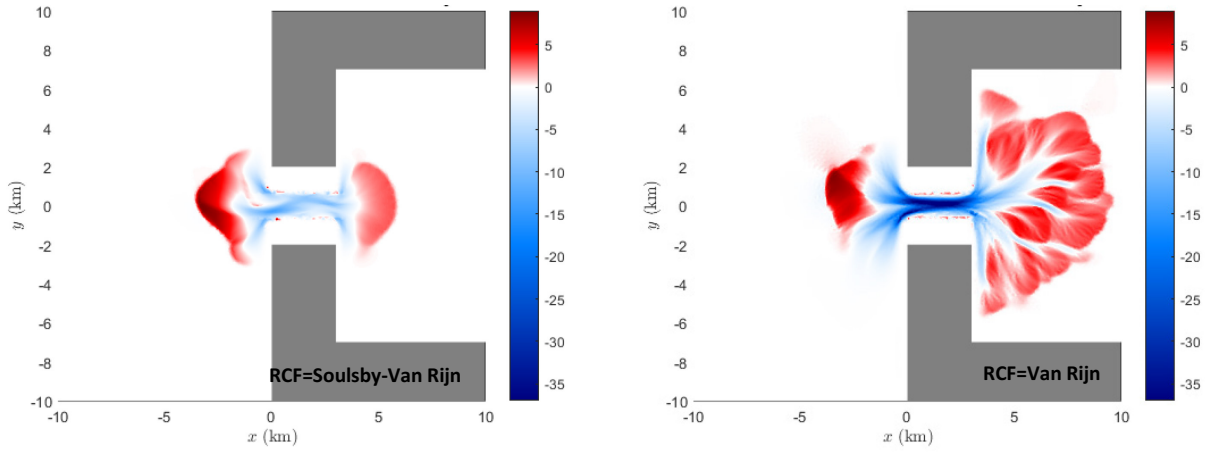

Bed slope effect

A sloping bottom increases bedload transport rate in the downslope direction reduces it in the upslope direction. In SISYPHE, a correction factor can be applied to both the magnitude and direction of the bed (or total) load transport rate, before solving the bed evolution equation.

For the magnitude correction, two different methods are available in SISYPHE depending on the basic concept of the bed (or total) load formula. The first method (SLOPEFF=1) is based on the Koch and Flokstra's formula (1981), according to which the transport rate is multiplied by a factor $[1- \beta(\partial Z_f/\partial s)]$, with s the coordinate in the current direction, Z_f the bed level, and β an empirical factor (BETA). This bed slope effect is then similar to adding a diffusion term in the bed evolution equation, which tends to smooth the results and reduces possible instabilities. Different values for BETA lead to different solutions. The higher the BETA coefficient the higher the diffusion of the solution will be. BETA = 0 means no magnitude correction. The second method for magnitude correction (SLOPEFF=2) is based on the method of Soulsby (1997), in which the threshold bed shear stress (critical Shields number) is modified as a function of the bed slope, the angle of repose of the sediment (default value in SISYPHE is 40°), and the angle of the current to the upslope direction. Since this method can be combined with threshold bed load formulas only, its effect on bed evolution was investigated coupled with Van Rijn's formula (ICF=7), while the suspended sediment transport was on. The results of this test a nice branched pattern in the back-barrier basin but both formulas and applying no magnitude correction results in big differences in the branching pattern.

For the correction of the transport direction the two different formulas are provided in SISYPHE, i.e. the formula of Koch and Flokstra (1981) (DEVIA=1), and the formula of Talmon *et al.* (1995) (DEVIA=2). Both formulas give a different branching pattern in the back-barrier basin.

Eddy viscosity and sediment diffusivity

So far in their sensitivity analysis Kolokythas et al. (2018) used a constant turbulence model with an eddy viscosity value of $\nu_t = 10^{-4}$ m^2/s^{-1}. The diffusion of suspended sediment was determined by constant in time and space diffusion coefficients in both x and y directions, i.e. $D_x = D_y$ (=D_{xy}) = 0.01 m^2/s^{-1}.

Figure 8 shows on the left side (a, c and e), bed level changes obtained using three different diffusion coefficients, i.e. D_{xy} = 0.01, 1 and 10 m^2/s^{-1}, respectively, after a simulation period of about 10 years. The general shape of the branching system in the tidal basin remains stable but the tidal channels are substantially altered; especially in the case of the highest D_{xy}, where 'capillary' branches show up at the endings of the larger scale channels. The combined impact of eddy viscosity and diffusion coefficients on the tidal inlet patterns is shown in the right column of Figure 8 (b, d and f), where eddy viscosity and diffusion coefficient values are, $\nu_t = D_{xy}$ =0.01, 1 and 10 m^2/s^{-1}, respectively. In general it was found that

eddy viscosity plays a more important role in the diffusion of the solution, which is getting more diffuse with increasing v_t values, as clearly shown in Figure 8(f). The diffusion introduced by higher eddy viscosity values makes the smaller tidal channels disappear. However smaller increase of v_t (see figure (b)) doesn't affect substantially the quantity of the channels in branching system even though the outline of pattern presents differences compared to the one of $v_t = 10^{-4}$ m^2/s^{-1}. This might be due to the presence of numerical diffusion. The numerical diffusion scales with the grid resolution.

Figure 8 – Bed level change [m] obtained after 9.6 years using three different diffusion coefficients [m2/s-1] (a,b: Dxy = 0.01; c, d: Dxy = 1; e, f: Dxy = 10)

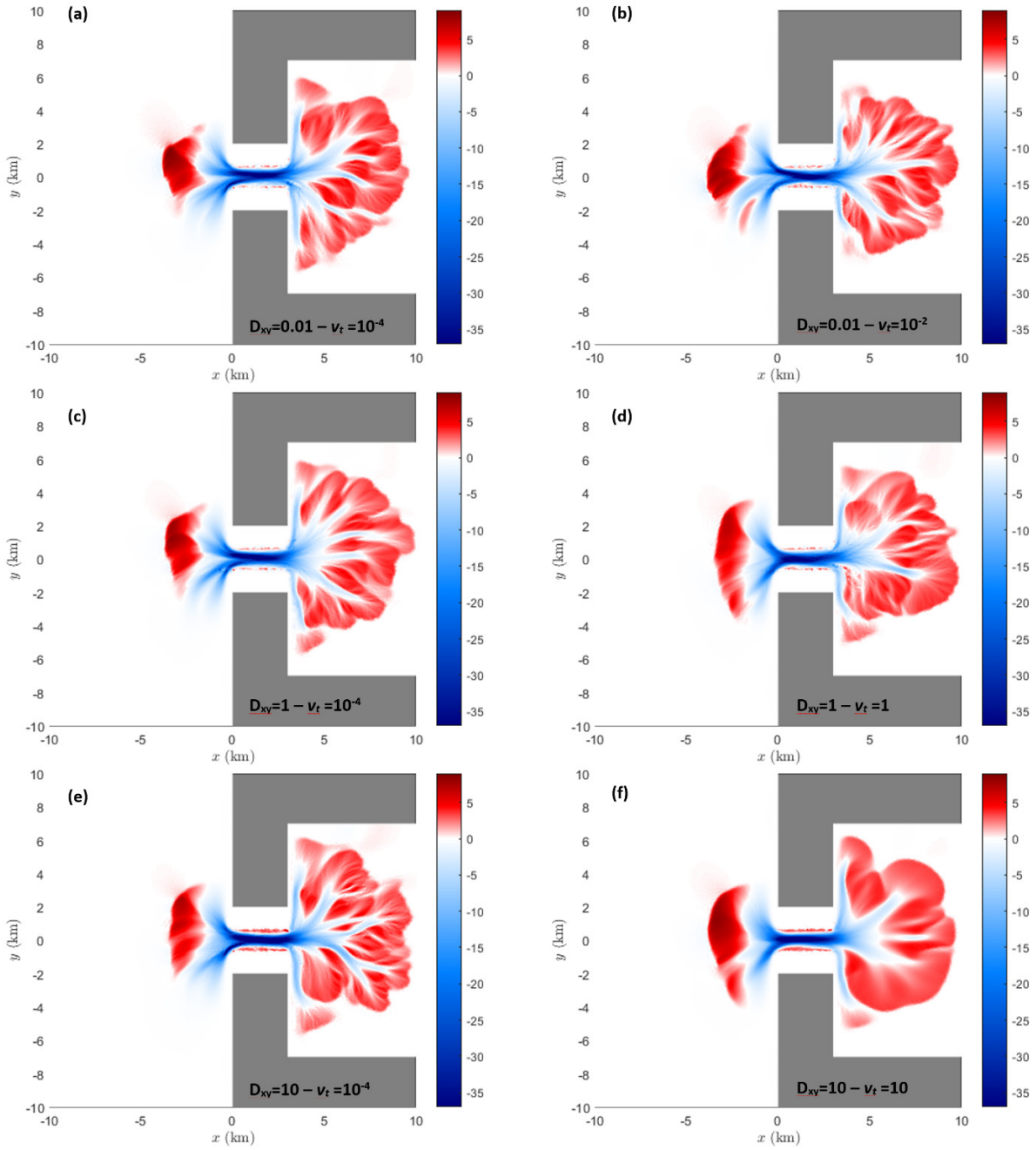

in the left column figures, eddy viscosity has the default (for this study) value $v_t = 10^{-4}$
in the right column figures, eddy viscosity values [m^2/s^{-1}] coincide with the diffusion coefficient values, i.e. (b) $v_t = 0.01$, (d) $v_t = 1$ and (f) $v_t = 10$. Van Rijn's bed load formula and sediment suspension are considered.
The figures zoom at the area of the tidal inlet (copy from Kolokythas et al., 2018).

Grid structure

The numerical results are very sensitive not only to the element size but also to the grid structure. Tests with the use of two hybrid grid structures consisting of structured (right) triangles at the tidal inlet area and unstructured triangles far from the area of interest, showed significant differences at the bed evolution in the tidal inlet area. The branching pattern changed.

2.2 A sand model for evaluation of the sediment strategy for the lower Sea Scheldt (Vos et al., 2016)

The hydrodynamics are computed with a 2D D3D model cut out of the 3D NEVLA model (Maximova et al., 2013). The study area is the Lower Sea Scheldt so the downstream boundary is located downstream Ossenisse. The upstream boundary is located at Tielrode on the Sea Scheldt and Terhagen on the Rupel. The computational grid was 3x3 refined based on the original NEVLA model. The smallest length scale is about 15 m. For the downstream boundary a water level was imposed. For the two upstream boundaries a discharge time series was imposed. All data was extracted from a simulation with the original NEVLA model. A time step of 7.5 s was used. Secondary flow was turned off. Horizontal eddy viscosity was set to 1 m^2/s. There was no salinity and no wind active in the model. Bottom roughness was set using a Manning coefficient of 0.025 $s/m^{1/3}$.

The sediment model uses two fractions: one sand and one mud. The density of the sand fraction was set to 1600 kg/m^3 (2650 kg/m^3 specific density and 40% porosity). A d50 value for sand of 150 µm was chosen. This value was chosen based on samples taken during 13 hour measurement campaigns in the Sea Scheldt (Plancke et al., 2014). The initial sand concentration in the water column was constant over the entire model domain and was equal to 0.1 kg/m^3. On the upstream and downstream boundaries a constant sediment concentration was imposed based on measurements (Vandenbruwaene et al., 2015) and equal to 0.05 kg/m^3. It was made sure that at the boundaries there was no excessive sedimentation nor erosion. The bottom of the model contains the same sediment in a layer with a thickness of 5 m. The reference simulation was performed using the Van Rijn (1993) sediment transport formula.

A sensitivity analysis was done by varying the d50 value of the sand, changing the sediment transport formula, adding secondary flow, adding salinity, adding more fractions. The outcome of this analysis is briefly summarized here. Smaller d50 values give higher transport rates. d50 values of 100, 150 and 200 µm were tested. Different values performed better for different periods in the tidal cycle. Using secondary flow made the model unstable and was not further tested. Adding salinity in the model had almost no effect on sediment transport rates. Horizontal salinity gradients can affect the estuarine recirculation and tidal asymmetry. This will disturb the theoretical logarithmic velocity profile. However, in a 2D depth averaged model these effects are not taken into account and as such don't result in large changes in sediment transport rates. When using the transport formula of Soulsby/Van Rijn the sediment transport rate increase significantly. At Liefkenshoek the maximum ebb rates increase with 300 g/m/s and at maximum flood this increase towards 600 g/m/s. When using Engelund and Hansen transport equation transport rate also increase compared to the default Van Rijn (1993) equation, but are not as high as the Soulsby/Van Rijn transport formula. For the thickness of the erodible sediment layer on the bottom, lithological maps were used and the thickness of the bottom layer was adjusted for each node in the model separately based on lithological information. Using multiple fractions (3 sand fractions + 1 mud fraction) resulted in lower transport rates. One of the reasons was that all the available sediment on the bottom was eroded within the simulation time.

After these results Vos et al. (2016) choose the following parameter values for their sand model: d50 was chosen equal to 150 µm because it was closest to measured samples from the Sea Scheldt. Salinity and Secondary flow were omitted. Using multiple sediment fraction did not give better results and only consumed more computation time, so a single sand fraction was chosen. The sediment transport formula of Engelund and Hansen was chosen because based on literature (Van Dam, 2014) this formula was more

suited for morphological modelling of the Lower Sea Scheldt. the thickness of the bottom layer varied based on a lithological map for the Lower Sea Scheldt. The authors state that these parameters give good predictions of sand transport rates for the Lower Sea Scheldt.

Longer morphological simulations revealed large differences in bathymetry result when using different sediment transport equations.

2.3 Morphodynamic modeling using the Telemac finite-element system (Villaret et al., 2013)

This paper describes the capacity of TELEMAC to be used for morphodynamic studies. It elaborates on the different modules involved (TELEMAC-2D, TELEMAC-3D, SISYPHE and TOMAWAC) and describes three validation cases.

For bed load transport semi-empirical transport formulas from literature are programmed in the code. The total bed shear stress τ_0, calculated based on the hydrodynamics, includes the effects of bedforms averaged over the mesh size. This can be corrected for local skin friction of the bed. The bedload transport rate is calculated as a function of the excess bed shear stress, i.e. the bed shear stress above the critical bed shear stress. The effect of a longitudinal or a transverse bed slope on the direction and magnitude of the sand transport rate is accounted for by the implementation of Koch and Flokstra (1981). The deviation of the transport direction is determined after Talmon (1992). In 2D models the method of Engelund (1974) has been programmed to reproduce transverse bed evolution in curved channels. The bottom shear stress is then modified in direction and magnitude depending on the water depth h and the radius of curvature R. The radius, unknown in the model, is substituted using a formulation for the slope of the free surface, $\partial Z_s/\partial n$, such that $g(\partial Z_s/\partial n)=\alpha' U^2/R$ in bends, with Z_s the free surface elevation and n the transverse direction. The correction factor α' is the only calibration parameter and should be chosen between 0.75 (presence of bed forms) and 1 (flat bed). This is demonstrated in the first validation case shown later.

For suspended load the suspended sediment concentration can be treated as a passive scalar in TELEMAC-3D by solving a classical transport/diffusion equation with an additional vertical advection term to represent the effect of the gravitational settling velocity. In SISPYPHE the depth averaged forms of these equations are solved with the source term being the net erosion (E) minus the deposition (D) flux. the erosion flux is then expressed in terms of 'equilibrium' reference concentration, and the deposition flux is calculated as the product of settling velocity (W_s) and the near bed concentration. In the 2D model, the advection term is corrected to account for the vertical distribution of velocity and concentration, leading to a global reduction in the convection velocity.

The variation of the bed elevation is derived from a mass balance, expressed in the Exner equation:

$$(1-p)\frac{\partial Z_f}{\partial t} + Div\left(\overrightarrow{Q_b}\right) + (E-D) = 0 \qquad 2.1$$

where p is the bed porosity, Z_f is the bottom elevation and Q_b is the solid volume transport rate (bed load) per unit width. Under quasi equilibrium flow conditions, a total load transport formula can represent both bed load as suspended load components. Equation 2.1 then becomes:

$$(1-p)\frac{\partial Z_f}{\partial t} + Div\left(\overrightarrow{Q_t}\right) = 0 \qquad 2.2$$

Validation case 1 describes the flow and sediment transport in a curved channel and corresponds to laboratory experiment no. 4 of Yen and Lee (1995). Recirculating cells in the transverse direction are responsible for the occurrence of meandering, which is one of the most important processes in river morphology. When SISPYHE is coupled with TELEMAC-2D or in 2D models in general, the effect of secondary currents on the direction and magnitude of the sand transport rate needs to be parameterized. In SISYPHE the method of Engelund (1974) as described above is used. In the validation case the evolution of the bed in a 180° channel bend was investigated under unsteady flow conditions with non-uniform

sediment. The width of the flume was 1 m and the radius of curvature was 11.5 m. Starting from a horizontal flat bed in the transverse direction with a longitudinal bed slope of 2%, a typical bank-cross section with scour at the outer bank and deposition at the inner bank was formed without imposing any sediment discharge upstream. Starting from an initial flow rate of 0.02 m^3/s (corresponding to incipient motion), the flow discharge was linearly increased during 5h up to 0.053 m^3/s and then progressively decreased back to its initial value. The bed material consisted of sand with a mean diameter of 1 mm and a uniformity coefficient $\sqrt{d_{84}/d_{16}}$=2.5, where d_{84} and d_{16} are representative grain sizes. In the simulation the sediment was assumed to be uniform (d_{50} = 1 mm). With this simplification the focus of the simulation was on the validation of the secondary current approach. The bed load formula of Meyer-Peter and Muller (1948) was applied with a critical Shields parameter of 0.033, corresponding to the mean grain size. The bed roughness was taken 3 times the mean diameter (k_s = 0.003 m), which corresponds to flat bed conditions. for the sloping bed effect, the approach of Koch and Flokstra (1981) was used for the magnitude and the approach of Talmon (1991) was used for the direction. the parameter α' was set to 1 because no bed forms occurred during the experiment. the simulation results were in good agreement with the measurements for the bed evolution despite the fact that sand grading effects were not taken into account (see Figure 9). The transverse slope occurring in the mid cross section is reproduced perfectly well, but further downstream the transverse slope at cross section 180° is overestimated by the simulation. Without the secondary flow current parameterization (α'=0) no transverse slope would occur, which highlights the importance of transverse currents.

Figure 9 – Measured (isolines) and calculated (colored) contours of the bed evolutions normalized by the initial water depth H_0 (=0.0544 m). (After Villaret et al., 2013)

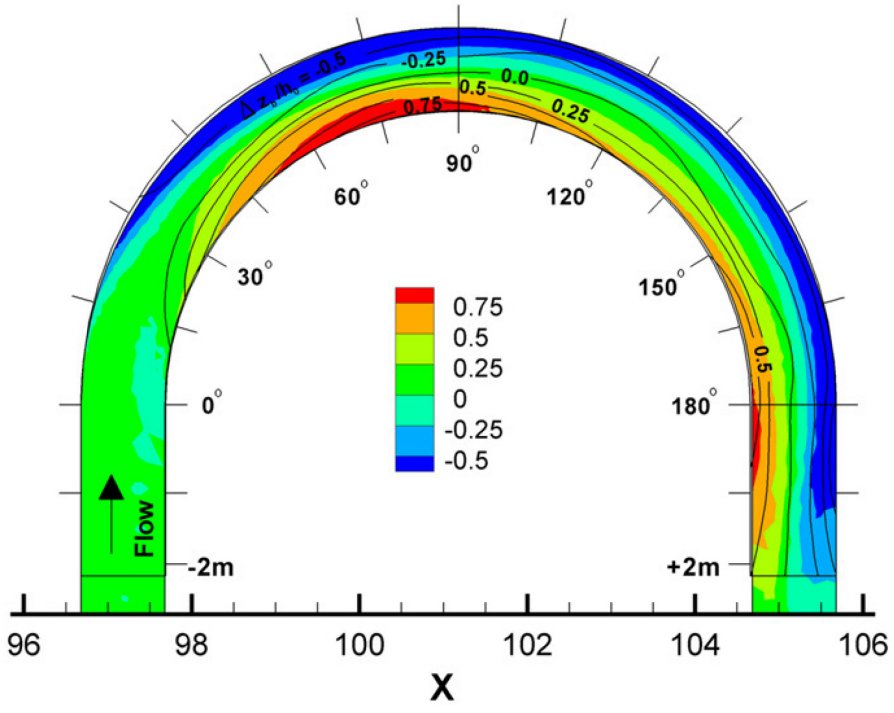

The second validation case was sand transport in a channel with a contraction. The third validation case was a litoral case to underline the effect of waves on coastal sand transport. Both cases are less relevant for this study and are not further discussed here.

In conclusion, the paper of Villaret et al. (2013) shows with validation cases that the sediment transport module SISYPHE is capable of reproducing the most important sediment behaviour.

2.4 Suggested parametrization of sand transport in SISYPHE

Based on the experience and sensitivity analysis done by Vos et al. (2016) using multiple fractions of sand did not improve the transport results of the model. They concluded a single fraction with a d50 value of 150 µm performed best for the Sea Scheldt. The d50 value choice was based on results from 13 hour measurement campaigns along the entire Sea Scheldt (Plancke et al., 2014). As transport formula they used the Engelund and Hansen total transport equation. This equation was also chosen by Kolokythas et al. (2018) after a sensitivity analysis. Vos et al. (2016) also tried Van Rijn's formula but found no significant improvement. Kolokythas et al. (2018) found that Engelund and Hansen performed better for a tidal inlet case than Van Rijn's formula. But other studies use the Soulsby-Van Rijn transport formula (Soulsby, 1997) to simulate sand transport in estuarine environments. Robins and Davies (2010) use this formula with a uniform sand grain size of 250 µm to simulate sand transport in the Dyfi estuary in the UK. Huisman et al. (2018) also used the Van Rijn transport equation (2007) to model the sand transport of five different fractions of the Sand engine in a Delft 3D model environment. More examples can be given, but for estuarine sand transport modeling usually Engelund and Hansen or the Van Rijn equation is used.

3 The Hydraulic Model: Scaldis 3D

The Scaldis model was developed within the framework of the project 13_131 Integrated Plan for Upper Sea Scheldt (Smolders et al., 2016). There was a need for a numerical model with higher mesh resolution in the upstream part of the Scheldt estuary. An unstructured mesh has the advantage to be very flexible in changing mesh resolution in specified areas. Therefore the Scaldis model was developed in the TELEMAC software, which is based on a finite element method.

The computational grid includes the Belgian coastal zone, extended to Dunkirk in France and Westenschouwen in the Netherlands. The grid includes the Eastern Scheldt as well. The mesh resolution varies between 400 and 150 m in this part of the model. In the Western Scheldt and estuary mouth area the grid resolution increases towards 120 to 80 m. The grid includes all tributaries reaching as far as the tidal influence. The grid resolution keeps increasing all the way till the upstream boundary in Merelbeke where it is 5-7 m. All flood control areas of the Sigma Plan are included in the grid. The 2D grid consists of 459 692 nodes. The 3D mesh consists of prisms eventually cut into tetrahedrons and is automatically constructed from the 2D mesh. A sigma transformation is used for the vertical location of these 5 layers. Layer 1 is the bottom layer and the following layers are always situated on 0.12, 0.30, 0.60 and 1.00 fraction of the water depth.
The bathymetry is interpolated from measured data from 2013 or the closest date available. For more detailed information we refer to the calibration report of the Scaldis model from Smolders et al. (2016).

There are 9 liquid boundaries in the Scaldis model. The downstream boundary is located in the North Sea. A water level is imposed on this boundary. This boundary contains 469 nodes. On every node a water level time series with 10 minute interval is imposed. These time series are extracted from the regional ZUNO model of the southern North Sea. A correction of the harmonic components was calculated based on the comparison of the harmonic components of the ZUNO results and measurements over a period of 1 year (Maximova et al., 2015). Differences in harmonic components (ZUNO vs. measurements) are found for stations in the Belgian and Dutch Coastal zone for the M_2, M_4, S_2 phases and the Z_0 component. After extraction of time series from the ZUNO model the time series of the boundary conditions of the Scaldis model are “harmonically corrected” with the obtained correction terms (+4° for M_2, -6° for M_4, +7° for S_2 phase and -21 cm for Z_0). This means that the time series are decomposed in harmonic components and a residual term. The harmonic components are corrected, and the signal is resynthesized. The subroutine BORD3D.f was changed to read and impose the appropriate time series for each boundary node.

There are 8 upstream liquid boundaries with prescribed discharges. Measured daily average discharges are available as upstream boundary conditions for Merelbeke (Melle), Dender, Zenne, Dijle, Kleine Nete, Grote Nete, and channel Ghent – Terneuzen. The values for the channel Ghent-Terneuzen were taken downstream the weir of Evergem. This location was used as a proxy. For the channel of Bath hourly discharge measurements were available. In this time series the small negative values were set to zero for stability reasons. All the other daily averaged discharge values for the other upstream discharge boundaries were then hourly interpolated. So all discharge boundaries have hourly discharge values. For each simulation these time series per upstream boundary are given in a liquid boundary file.

Wind influence is not included in the hydrodynamic model. Wind effects showed very minor interaction with the spring-neap tide hydrodynamics inside the estuary. The wind effects on the North Sea are taken into account in the model boundary conditions.

Salinity is applied as an active tracer. This means that density effects are taken into account in the model. time series with 10 minute interval are imposed on the downstream boundary. The salinity values are generated from the CSM-ZUNO model train. Salinity boundary values in the Scaldis model were corrected based on the comparison of the simulated and measured salinity time series at Vlakte van de Raan (located in the larger mouth area of the Scheldt Estuary). The ZUNO model underestimates the salinity values in the

area of interest and a salinity correction at the boundaries was necessary. The correction is specific for a specific time period. The difference between the daily averaged measured and modelled values was used for correction of the salinity time series for the downstream boundary condition. On the upstream boundaries the salinity boundary conditions are set to zero for the incoming discharges. No salinity is entering the domain through these boundaries in the Scaldis 3D HD model. The model starts from an initial salinity field: a map is made based on a combination of salinity measurements (Western Scheldt) and corrected model results from ZUNO (coastal area). This initial salinity map is read at the start of a simulation by a modified subroutine fonstr.f. The values of the 2D map are copied to the other four layers in the model.

The model runs with a time step of 4 seconds. A cold start is done with a constant water level throughout the entire model domain and the boundary imposed water levels and discharges are smoothed for the first tidal cycle. Manning's equations is used for the bottom roughness and these values vary along the estuary and were used to calibrate the hydrodynamic model. Negative depths are clipped to zero with flux control to keep the model stable. The RANS equations are solved also on the tidal flats with corrections. As a vertical turbulence model the mixing length model of Nezu and Nakagawa was used. The horizontal turbulence model is a Smagorinski model. Coriolis is activated with a coefficient value of 1.13522E-04.

4 Calibration & Validation data

4.1 Measurement campaigns 2014

The necessary data to allow model validation were not present at the start of this project. Therefore, eight measurement campaigns were done in 2014 in the Sea Scheldt: Liefkenshoek[1], Oosterweel, Kruibeke, Driegoten, Dendermonde, Schoonaarde, Schellebelle and Terhagen. For the locations along the estuary see Figure 10. The results of these measurement campaigns were reported in Plancke et al. (2014). In this section a brief summary is given concerning the sand transport results.

To measure sand transport a Delft bottle was used (see Figure 10). This is a bronze bottle-like core with in front of it a small opening to let water in and in the back four small openings to let the water back out. Because of the bottle shape a pressure difference arises between the front and the back. This causes head losses inside the device that are the same for different flow velocities outside. Inside the bottle the water has to travel through a labyrinth in which the flow velocity decreases. This decrease in velocity traps sediment particles larger than 50 µm. The sampling time can be adjusted to the flow velocity and sediment load of the river so that a sample would generate a representative amount of sediment. The “filtered” volume of water can be very large if the sediment load is small.

Figure 10 – Delft bottle on frame (left) and hung (right) (figure from Plancke et al., 2014)

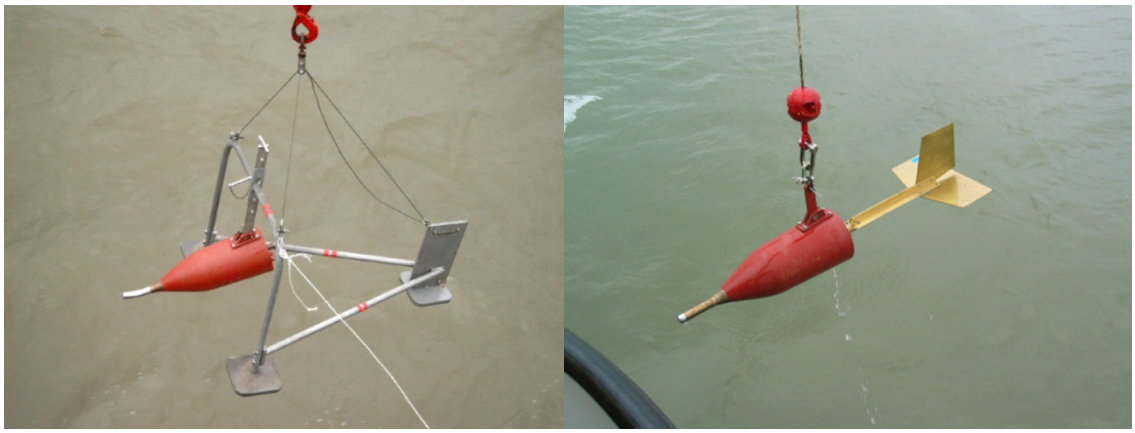

When the Delft bottle is taken back out of the water, its content is poured through a funnel into a measuring tube. The sediment is allowed to settle during three minutes before the volume is read from the tube markings. Because the inlet opening of the bottle and the sampling time is known, the volumetric sediment transport can be calculated. Assumptions for porosity and density of the sediment still have to be made to calculate mass transport. For mud and sand a porosity of 0.9 and 0.5 respectively was chosen. Sediment density was taken to be 2650 kg/m³. After measurement the sample is poured into a container to bring it to the lab for grain size analysis. The Delft bottle can be used close to the bottom, mounted on a frame; or can be used hung from a cable to measure transport in suspension. In the last case a tail is mounted to the bottle to keep it aligned against the flow. In the measurement campaigns the Delft bottle

[1] The vessel was not anchored well during this measurement campaign and had to move several times and even go to the other bank of the river. This makes the measurements useless for use in model calibration/validation.

was mounted on a frame to measure at 0.2 and 0.4 m above the bottom and a second bottle was hung from a cable to measure suspended transport 1.3 and 2.3 m above the bottom.

At every measurement location a bottom sample was taken using a Van Veen sampler. Samples were used to determine grain sizes. This sampling method loses usually the finer fraction of sediment when winching up the device.

Sediment transport was measured at four locations along the vertical, but these measurement where done consecutively and not simultaneously. A total sediment transport over the vertical was calculated. To do so the measurements were interpolated to get a total transport value every 30 minutes. The following steps were taken to calculate the total transport:

- Q_s(t= n x 30'): linear interpolation of measured transports of the different vertical positions over time to get transport values for all vertical positions at moment X, i.e. every 30 minutes. If no measured value was available in the time frame [X-15', X+15'] , no value for that position was taken into account for moment X.
- Q_s^{rel}(z) [rel. = Q_s(z) / Q_s(z = B+ 0.2 m)]: A vertical profile was fitted using exponential regression on the interpolated relative transport values. This determines the ratio of the transport values at 0.4, 1.3 and 2.3 m to the transport at 0.2 m above the bottom. The regression was done for each location separately, based on all time steps and all available measurements, so that it delivers one relative vertical sediment transport distribution.
- Q_s(z,t): the total transport is calculated by integration of the vertical profile (exponential curve from step 2). For the first 0.1 m above the bottom a constant sand transport was assumed (the value on the exponential curve at 0.1 m above the bottom. A different bottom level was taken for ebb and flood calculations because of the turning of the ship around slack (mooring was done on 1 anchor). The actual water levels were used for the calculations.

Figure 11 – Map of the Scheldt estuary with main tributaries and most important locations

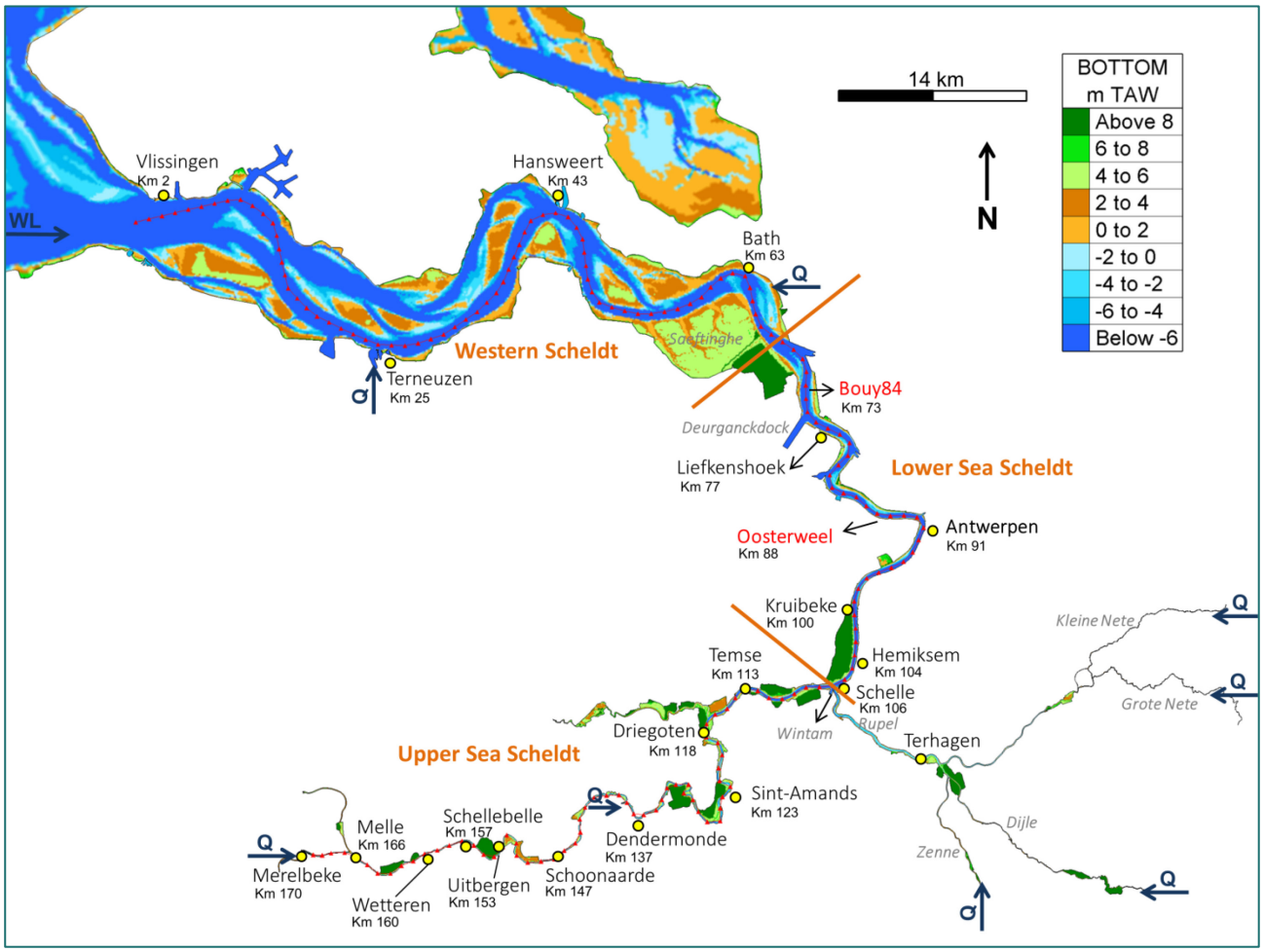

The calculated total transport for the different measurement campaigns is shown in Figure 12. This figure shows overall very high transport values for locations Schoonaarde and Driegoten and a very high peak in sediment transport for Oosterweel and Kruibeke. The transport rates are very high up to almost 5000 g/s/m for Driegoten. Grain size analysis showed a dominance of silt/mud (d50 < 63 µm at the moment of peak transport)[2].

At every location a bottom sample was taken and during the campaign different samples coming from the Delft bottle were analyzed for grain size distribution. The results for the bottom samples are shown in Figure 13. There was no bottom sample taken at Driegoten. The results show that the bottom in the lower Sea Scheldt (Kruibeke, Oosterweel, Liefkenshoek) has very fine sands. In the Upper Sea Scheldt (Dendermonde, Schoonaarde and Schellebelle) the D50 grain size confirms a sandy bottom. However when looking at the results for grain size distributions from the samples from the Delft bottle, shown in Figure 14, it can be seen that a lot of mud is present in these samples and that a large part of the sediment transport is in fact mud transport. The sand fraction (d > 63 µm) in the samples from the Delft bottle hung was in the same order of magnitude as the fine sediment in the bottle (d50 ~ 70 µm). Figure 14 also shows samples taken from the water column with a pump, also called suspension samples. These samples show D50 values that are even lower as the Delft bottle hung. The Delft bottle is designed to filter out sand particles and let the small size particles leave from the back of the bottle, therefore showing a larger D50 values in sampled grain size.

[2] Where this peak occurs near slack high water, results are biased by fine sediment travelling through the Delft bottle and settle in the bottle at low flow velocities.

The model only simulates sand transport and not the total sediment transport calculated before and shown in Figure 12. Therefore, all measured sediment transport values were corrected with the sand fraction in every sample. The sand fraction from samples, from which no grain size distribution was measured, was interpolated between samples from which grain size distribution was measured (Plancke et al., 2018). The total sand transport over the vertical is then compared with model results. To determine a good location/node in the model to compare with the measurements, the water depth and flow velocity at the location of the measurements was taken into account. A comparable tide was selected from the model results based on high and low water levels (comparable to high and low water levels during the measurements). The results are shown in section 5.5.1 of this report.

Figure 12 – Calculated total sediment transport for the different locations of the measurement campaign.

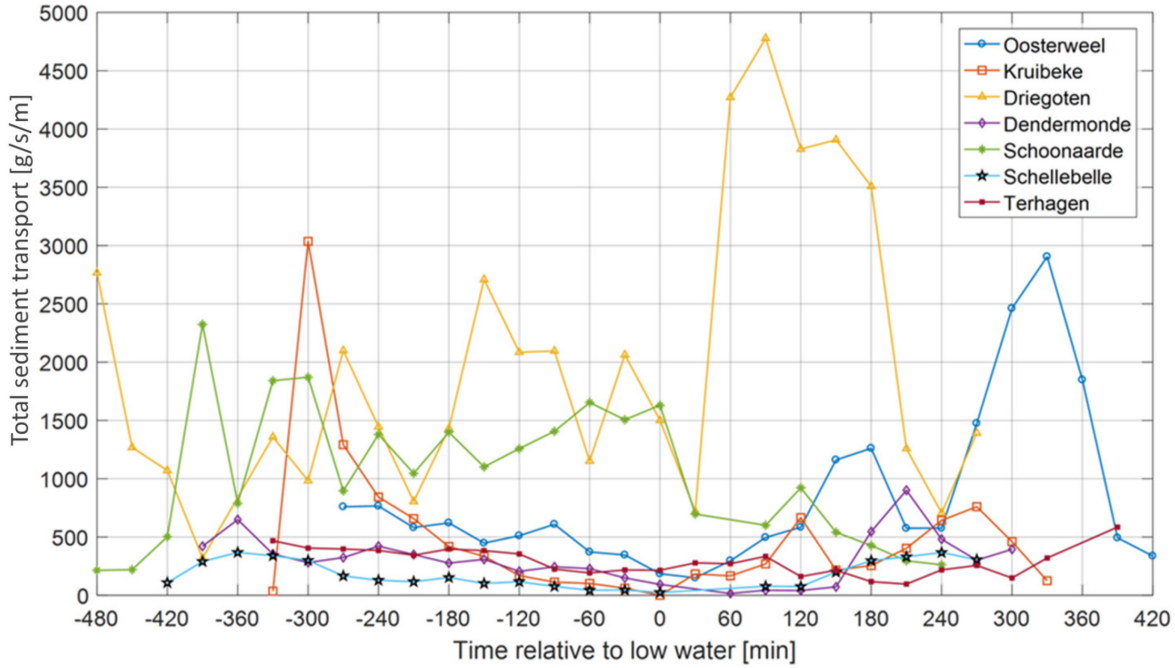

Figure 13 – overview of characteristic grain sizes of bottom samples from the different measurement campaigns.

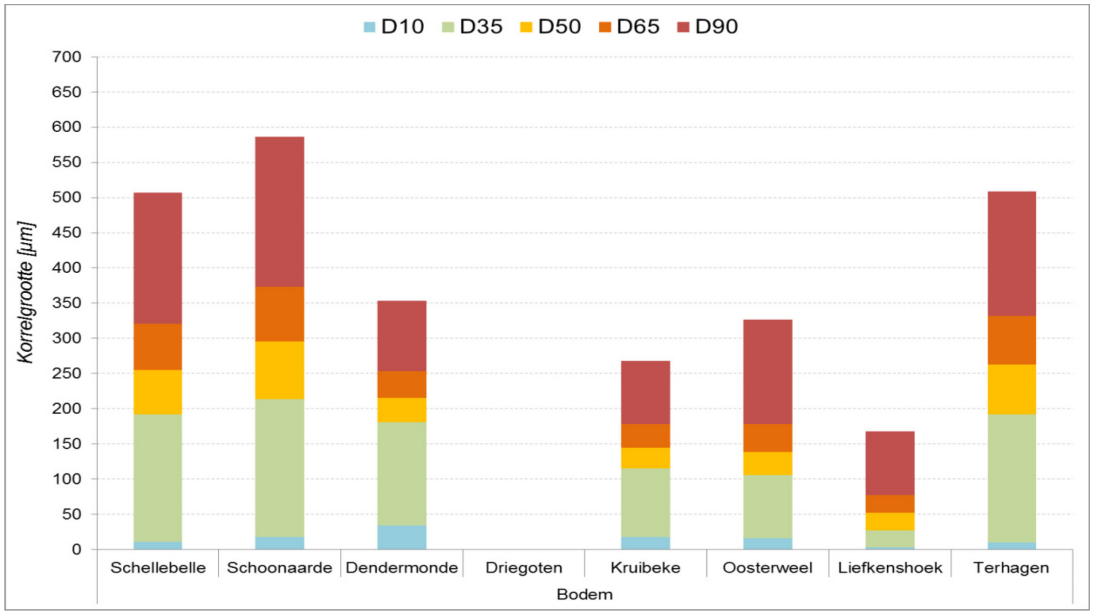

Figure 14 – Overview of characteristic grain sizes of samples taken during flood (frame above) and ebb (frame below) at the different measurement campaigns with the Delft bottle on frame (DBF), the Delft bottle hung (DBH) and suspension pump samples.

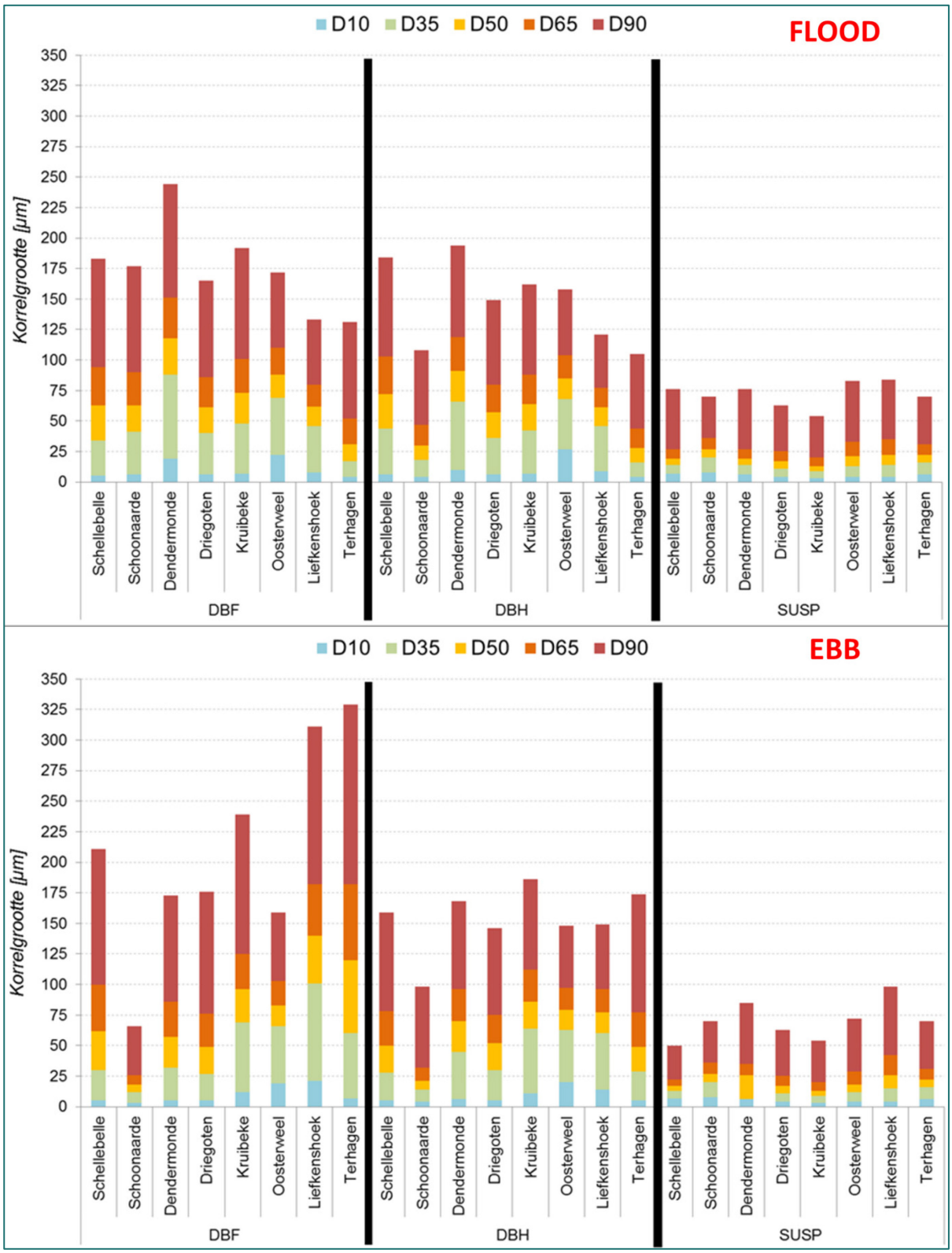

4.2 Calculated Sediment balance for Sea Scheldt (Vandenbruwaene et al., 2017)

Vandenbruwaene et al. (2017) calculated a sediment balance for the Sea Scheldt, Rupel and Durme for a period between 2001 to 2010. A balance was made for different large areas, cells, and sediment transport over the boundaries of these cells was calculated. A distinction was made between sand and mud transport. The calculations were based on changes in bathymetry, ecotopes and the lithological information of these ecotope areas. Anthropogenic influences like dredging and dumping, sand mining, fluxes to harbor docks and de-embankments were also taken into account. A sensitivity analysis demonstrated the robustness of the results and the transport directions.

The sand transport model will give results over the same cell boundaries for a full spring-neap tidal cycle. The net transport over this period will be scaled up to a yearly transport rate. The sand transport calculated by Vandenbruwaene et al. (2017) will be brought back to a yearly transport rate by dividing the result by 10 (period of ten years 2001-2010). The results from the model give the volume of pure sediments and pore spaces are not taken into account. The results given by Vandenbruwaene et al. (2017) are volumes taking into account the pore spaces. For sand a porosity of 0.5 is assumed and the values from Vandenbruwaene et al. (2017) are then multiplied with this porosity factor so that they can be compared with the model results. Results are compared in magnitude and direction in section 4.6.2 of this report.

5 Model setup

5.1 Introduction

This chapter describes the setup of the sand transport model within the SISPYHE module of the TELEMAC software suite. The sediment transport module SISPYHE is coupled with the TELEMAC-3D model Scaldis, described in the previous chapter. No changes were made to the calibrated Scaldis 3D hydrodynamic model.

Parameter choices for SISPYHE will be based partially on experience of previous projects and papers as shown in Chapter 2. We choose to use Engelund and Hansen total load equation for Sand transport. A uniform grain size is used with a d50 that is based on measurements (= 150 µm).

This chapter first describes the conceptual model and the equations that are implemented in the SISYPHE module. Then a section is devoted to measurements against which model results will be compared. This is followed by a section describing the choice of boundary and initial conditions.

5.2 Conceptual model in SISYPHE

5.2.1 Bed load transport

Bedload transport are particles that are transported over the estuary bed by rolling, sliding, saltation. SISYPHE solves the conservative law equation for sediment mass (= Exner equation):

$$(1-\lambda)\frac{\partial z_b}{\partial t} + \nabla Q_b = 0 \qquad 5.1$$

with Q_b the solid volume transport vector per unit width [m²/s], with components Q_{bx}, Q_{by} in the x and y direction respectively, z_b is the bottom elevation [m] and λ is the bed porosity. The bedload transport vector can be decomposed into x- and y- direction components as:

$$Q_b = \left(Q_{b_x}, Q_{b_y}\right) = (|Q_b|\, cos\alpha\ ,\ |Q_b|\, sin\alpha) \qquad 5.2$$

with Q_b the bedload transport rate per unit width, computed as a function of the equilibrium sediment load closure (or sediment transport capacity) and α is the angle between the sediment transport vector and the downstream direction (x-axis). The deviation of the bed load direction from the flow direction is mainly influenced by the bed slope and the presence of secondary flows.

The dimensionless current-induced sediment transport rate Φ_b is given as:

$$\overrightarrow{\Phi_b} = \frac{\overrightarrow{Q_b}}{\sqrt{g(s-1)d^3}} \qquad 5.3$$

with Q_b the bedload sediment transport per unit width [m²/s], $s=\rho_s/\rho$ the sediment relative density [-]; ρ_s the sediment density [kg/m³]; ρ the water density [kg/m³]; d the sand grain diameter (= d_{50} for uniform sediment distribution) [m] and g the gravity acceleration constant [m/s²], given by the keyword GRAVITY ACCELERATION (see Table 1)

Different transport formula for Φ_b are available in SISYPHE and are generally computed as function of the dimensionless Shields number θ:

$$\vec{\theta} = \frac{\mu\overrightarrow{\tau_b}}{(\rho_s-\rho)gd} \qquad 5.4$$

with τ_b the bottom shear stress [Pa] and µ the correction factor for skin friction.

Van Rijn (1984)

This formula (keyword: BED-LOAD TRANSPORT FORMULA = 7) is used in the sediment grain size range of d_{50} = [0.2 – 2] mm. The dimensionless current-induced sediment transport rate is given by:

$$\overrightarrow{\Phi_b} = 0.053 {D_*}^{-0.3} \left(\frac{\vec{\theta} - \theta_{crit}}{\theta_{crit}} \right)^{2.1} \quad 5.5$$

This formula calculates bedload transport only. It is calculated in the Fortran subroutine bedload_vanrijn.f.

Engelund and Hansen (1967)

This formula (keyword: BED-LOAD TRANSPORT FORMULA = 30) is used in the sediment grain size range of d_{50} = [0.2 – 1] mm. This formula is derived for river flow (Engelund and Hansen, 1967). The formula given by Engelund and Hansen estimates the total transport, $\vec{Q}_0$ [m²/s], in the direction of the flow velocity, $\vec{v}$:

$$\left|\vec{Q}_0\right| = \frac{0.05\alpha|v|^5}{\sqrt{g}s^2C^3d_{50}} \quad 5.6$$

where α is a calibration coefficient (order 1); $|v| = \sqrt{u^2 + v^2}$ is the magnitude of the flow velocity [m/s]; s =(ρ_s-ρ)/ρ is the relative density with ρ_s and ρ the sediment and water density, respectively [-] ; C is the Chézy friction coefficient [$m^{1/2}$/s] ; and d_{50} is the median grain size [m]. Furthermore, to account for the bed slope effects, the correction method of Flokstra and Koch, 1981, is available in SISYPHE (keyword: FORMULA FOR DEVIATION = 1) and multiplies the above equation by a factor:

$$\left|\overrightarrow{Q_b}\right| = \left|\vec{Q}_0\right| \left(1 - \beta \frac{\partial z_b}{\partial s}\right) \quad 5.7$$

where β is a bed slope coefficient (keyword: BETA = 1.3); s is the coordinate in the flow direction and z_b is the bed level.

This formula is implemented in SISYPHE in the subroutine bedload_engel.f. The formula is implemented as follows:

$$\Phi_b = C_{engel}\sqrt{(C_1 * TOB)^5 / \max(CF, 1.E-6)} \quad 5.8$$

whit

$$C_{engel} = 0.1\sqrt{s * g * d^3} \quad 5.9$$

and

$$C_1 = \frac{1}{(s*\rho*g*d)} \quad 5.10$$

and

$$CF = \frac{2n^2 g}{h^{1/3}} \quad 5.11$$

and

$$TOB = 0.5 * \rho * CF * |v|^2 \quad 5.12$$

where Φ_b is the dimensionless current induced sediment transport rate; TOB is the bed shear stress [Pa]; CF is the quadratic friction coefficient; s =(ρ_s-ρ)/ρ is the relative density [-]; g is the gravitational acceleration constant [m/s²]; d is the sediment grain size [m]; $|v| = \sqrt{u^2 + v^2}$ is the magnitude of the flow velocity [m/s]; n is the Manning friction coefficient [$m^{1/3}$/s]; h is the water depth [m]; and ρ is the water density [kg/m³]. CF can have a different formula depending on the type of friction coefficient that was chosen in the model. For Scaldis a Manning bottom friction coefficient was chosen and the corresponding formula for CF is given here (equation 5.11).

5.2.2 Modification of the magnitude and direction of bedload

Three key aspects are considered in SISYPHE: the effect of local bed slope, secondary flow effects on local bed shear stress and the partitioning of bed shear stress into components affected by skin friction and drag force from bed forms.

Correction of the direction of the sediment transport

To correct for the direction of sediment transport due to the presence of slopes, a sediment shape function f(θ) is introduced. This is a function weighing the influence of the transverse bed slope, expressed as a function of the dimensionless Shields parameter θ. There are two formulas to take this deviation from the flow direction into account (keyword: FORMULA FOR DEVIATION=1; see Table 1):

- formula of Koch and Flokstra (1980): $f(\theta) = \frac{2}{3\theta}$ 5.13

- formula of Talmon et al. (1995): $f(\theta) = \frac{1}{\beta_2}\sqrt{\theta}$ 5.14

in which β_2 is an empirical coefficient with a default value of 0.85. For dunes and bars in a laboratory channel Mendoza et al. (2016) found an optimal value for β_2 =1.6.

Correction of the magnitude of sediment transport due to the effect of the bed slope

The correction of the magnitude of the sediment transport in the direction of the sediment transport proposed by Koch and Flokstra (1980) is based on the modification of the bed load transport rate by a factor that acts as a diffusion term in the bed evolution equation (keyword: FORMULA FOR SLOPE EFFECT=1; see Table 1) :

$$Q_b^* = Q_b(1 + \beta \frac{\partial z_b}{\partial s}) \quad 5.15$$

where s is the flow direction and β is an empirical factor accounting for the streamwise bed slope effect (keyword: BETA=1.3; see Table 1).

The correction proposed by Soulsby (1997) is based on the modification of critical Shields parameter and is therefore only valid for threshold bedload formulas (like Meyer-Peter and Müller or Van Rijn (1984)):

$$\frac{\theta_{\chi cr}}{\theta_{cr}} = \frac{cos\psi\, sin\chi + \sqrt{cos^2\chi\, tan^2\phi - sin^2\psi sin^2\chi}}{tan\phi} \quad 5.16$$

where $\theta_{\chi cr}$ is the corrected Shields number for a sloping bed; θ_{cr} is the critical Shields number for a flat horizontal bed; ϕ is the angle of repose of the sediment (keyword: FRICTION ANGLE OF THE SEDIMENT=40; Table 1); χ is the bed slope angle with the horizontal; and ψ is the angle between the flow and the bed slope directions. (keyword: FORMULA FOR SLOPE EFFECT=2; see Table 1).

Skin friction correction

The total bed shear stress is a value that takes into account skin friction and bed form drag, but in SISYPHE only skin friction acts on the bedload. The shear stress due to skin friction is expressed as:

$$\tau' = \mu\tau_b \quad 5.17$$

with the total bed shear stress τ_b:

$$\tau_b = 0.5\rho C_f(U^2 + V^2) \quad 5.18$$

and with friction factor μ:

$$\mu = \frac{C_f'}{C_f} \quad 5.19$$

where C_f is the friction coefficient due to form drag + skin friction calculated in the hydrodynamics module and C'_f is the friction coefficient due to only skin friction. The latter is computed as follows:

$$C_f' = 2\left(\frac{\kappa}{\log\left(\frac{12h}{k_s'}\right)}\right)^2 \qquad 5.20$$

where κ is the von Karman coefficient (=0.40); k_s' is the roughness height = $\alpha_{k_s} d_{50}$ in which α_{k_s} is a calibration parameter (=keyword: RATIO BETWEEN SKIN FRICTION AND MEAN DIAMETER=3.0; see Table 1).

5.2.3 TELEMAC-3D versus TELEMAC-2D

In 2D TELEMAC-2D calculates the hydrodynamics and SISYPHE models the sediment transport, i.e. bed load and suspended load.

In 3D TELEMAC-3D models the hydrodynamics and SISYPHE models the sediment transport in 2D, bed load and suspended load. It is however possible to model the suspended transport in 3D. A module, called SEDI-3D, is available within the TELEMAC-3D code to model sediment transport by treating it like an active tracer. However, when TELEMAC-3D is coupled to SISYPHE, the transport model only uses the depth averaged flow conditions derived from the 3D model. Only when in the 3D model the Nikuradse model is used for the shear stress, the calculated bottom roughness from the hydrodynamic model is directly used for the bedload transport.

5.2.4 Overview of the relevant keywords to be used in SISYPHE for sand transport

All relevant keywords are listed in Table 2 in Appendix A accompanied by their default value and a short explanation as given in the SISYPHE dictionary file (SISYPHE.dico).

5.3 Model setup

5.3.1 Model parameters

The sediment module SISPYHE is coupled with the 3D hydrodynamic module TELEMAC-3D. No parameter changes were done in the hydrodynamic model Scaldis, described in Smolders et al. (2016).

In SISYPHE, the module is coupled with the hydrodynamics every time step. Engelund and Hansen was chosen to be the transport equation, based on the literature review in chapter 2. Suspended load transport is not activated in SISYPHE, but the Engelund and Hansen transport equation is a total load equation. The morphological factor is set to 1. The sediment grain size is equal to 150 µm. Only a single sediment fraction is taken into account over the entire model domain. There is an unlimited amount of sediment available in the model (= 100 m of sediment layer thickness).

The simulation runs for 15 days (a full spring-neap tidal cycle) and output is written to a results file every half hour. The time step is four seconds.

Slope effects are taken into account by default. Secondary currents is not active when coupled with a 3D hydrodynamic model. The 3D flow patterns are given to the SISYPHE module in a depth averaged way, because SISPYHE is a 2D module.

5.3.2 Boundary conditions

Sediment can leave the domain freely. No sediment enters the model domain through the boundaries. This is possible because only 15 days are simulated. To prevent the model from resulting into unwanted erosion at the inflow boundaries, a fixed bed elevation (zero evolution) was defined in the boundary conditions file (.cli). This can be achieved by assigning LIEBOR=5 for the inflow nodes (8th column in .cli file).

5.3.3 Initial conditions

The hydrodynamic model has two days to spin up. After these two days the model is started again from the last time step of the spin up simulation and the sediment module SISYPHE is coupled. A uniform sediment layer is available throughout the entire model domain. By default the initial sediment layer thickness is 100 m.

5.3.4 Dredging and dumping

No dredging or dumping activities are included in this model setup.

5.3.5 Bottom friction coefficient

In the hydrodynamic model a Manning bottom friction coefficient was spatially varied to calibrate the water levels and flow velocities in the model. By default the sediment module uses the bottom friction coefficient of the hydrodynamic module to calculate the bed shear stresses to estimate sediment motion. But during calibration of the hydrodynamic model the variation in bottom friction coefficient is used to compensate also for non-physical properties of the model, like numerical diffusion. Taking these values of the bottom friction coefficient would not be correct for sediment transport. Therefore a fixed value for the Manning bottom friction coefficient was used for the entire model domain for the sediment transport. In the subroutine coefro_sisyphe.f a fixed value for the bottom friction coefficient was introduced. The Manning coefficient was set to 0.02 $m/s^{1/3}$. In the subroutine tob_sisyphe.f changes were made to make sure the fixed bottom friction coefficient was used in the calculations of the bed shear stress.

The difference in sand transport between using a fixed Manning value for the entire model domain or using the Manning coefficient spatially varying from the hydrodynamic model is part of the sensitivity analysis that follows.

5.3.6 Morphological feedback

The sediment module calculates a certain sand transport and the related bottom changes. By default these bottom changes are updated in the bottom file of the hydrodynamic model every time step. But the focus of the sand transport model is on sand transport and not on morphology. Therefore the update of the bottom in the hydrodynamic model is switched off in the code. The mass balance and bottom changes are still recorded in the sediment module and are given as output, but the sand transport is always calculated based on the hydrodynamics with a fixed initial bathymetry.

6 Sensitivity analysis

A lot of parameters have already been tested in other projects and the result hereof are given in the literature review in chapter 2 of this report. So only a few extra tests were done within this report, mainly to see how the Scaldis model reacts on changes in D50 grain size, a different transport equation, on slope effects and on a different bottom friction coefficient.

The results are always shown in function of net sand transport over different transects along the estuary over the 15 day simulation period. For transect 23 (KM92), a transect up-estuary of the Antwerp region, time series of sand transport rate over the transect are also shown.

The default model parameters were described in the section above.

6.1 Grain size (D50)

The D50 value for grain size was altered from 150 µm to 200 µm to 250 µm. The Engelund and Hansen transport equation does not have a threshold value for incipient motion (equation 5.6), so increasing the grain size will not increase any threshold for that. In equation 5.6 the D50 value is in the denominator so that an increased grain size will result in a decrease in transport. Figure 15 shows the net sand transport over a period of 15 days over different transects along the Scheldt estuary for the three different D50 values. A positive net transport value means that the transport is directed downstream (ebb dominated) and a negative value means that the transport is going upstream (flood dominated). The figure shows that the larger D50 values give lower net transport. Figure 16 shows the time series of the 15 days simulation for transect 23, which is located around km 92 (up-estuary of Antwerp) from the estuary mouth at Vlissingen. In the time series it is also clear that the larger D50 values have a lower sand transport.

Figure 15 – Effect of D50 grain size value on net sand transport over different transects along the Scheldt estuary.
A positive net transport is transport in the downstream direction. A negative net transport is transport in the upstream direction.

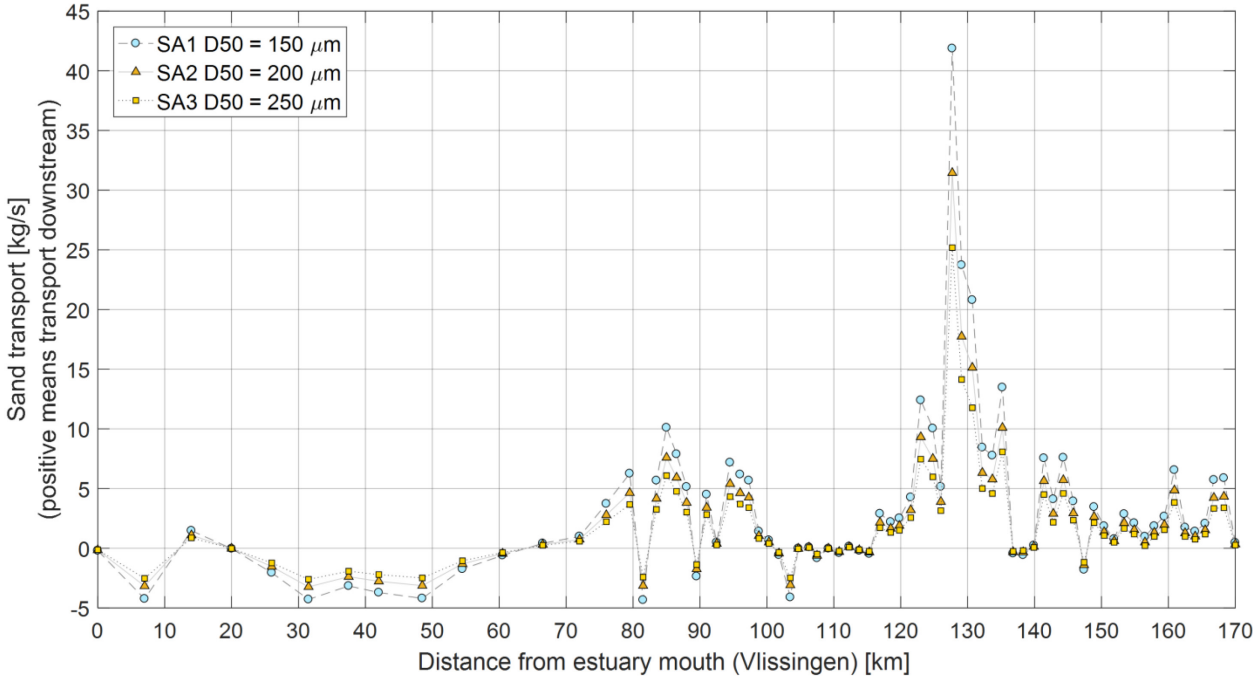

Figure 16 – Time series of sand transport over transect 23 at 92 km from the estuary mouth at Vlissingen for different D50 grain size values. A positive value means downstream transport and a negative value means an upstream transport.

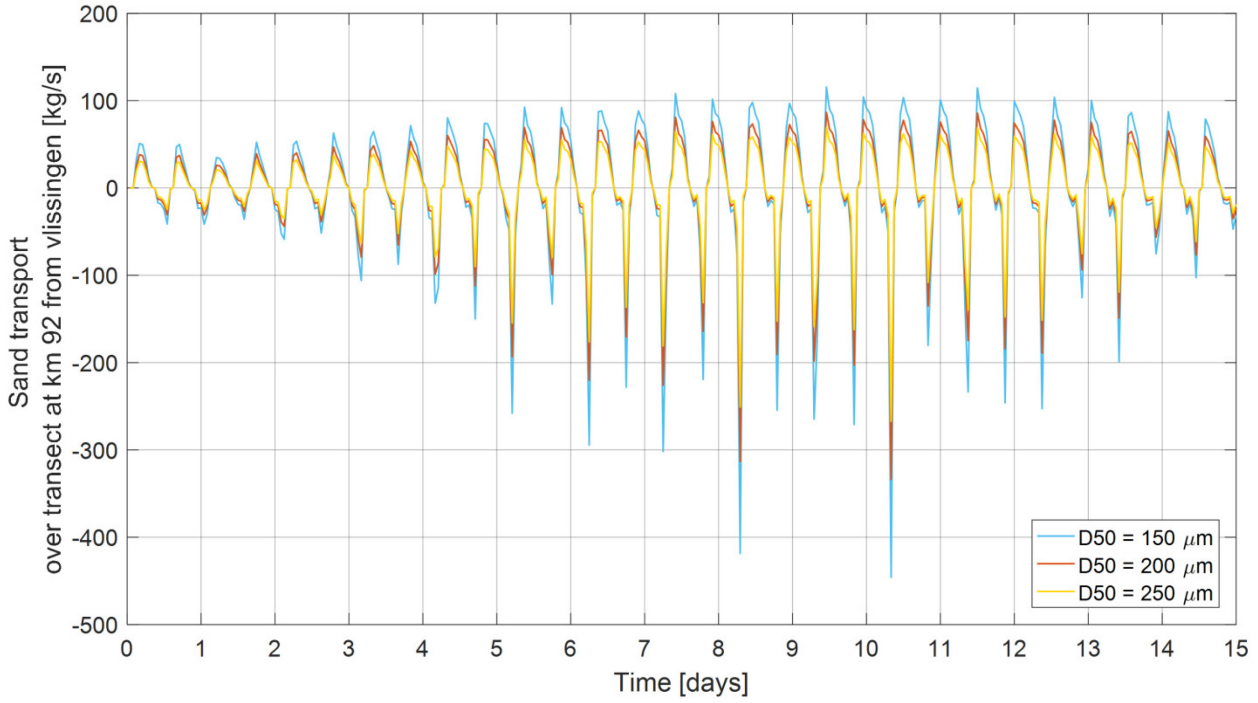

The net transport direction is a result of the integration of the time series of sand transport for a certain transect. Figure 17 shows in detail the daily inequality of a spring tide resulting in a net transport downstream (net positive transport = transport downstream). For this double tide there is a net transport of 327 m^3 of sand downstream.

Figure 17 – daily inequality of a spring tide resulting in a net ebb (positive) dominated sand transport

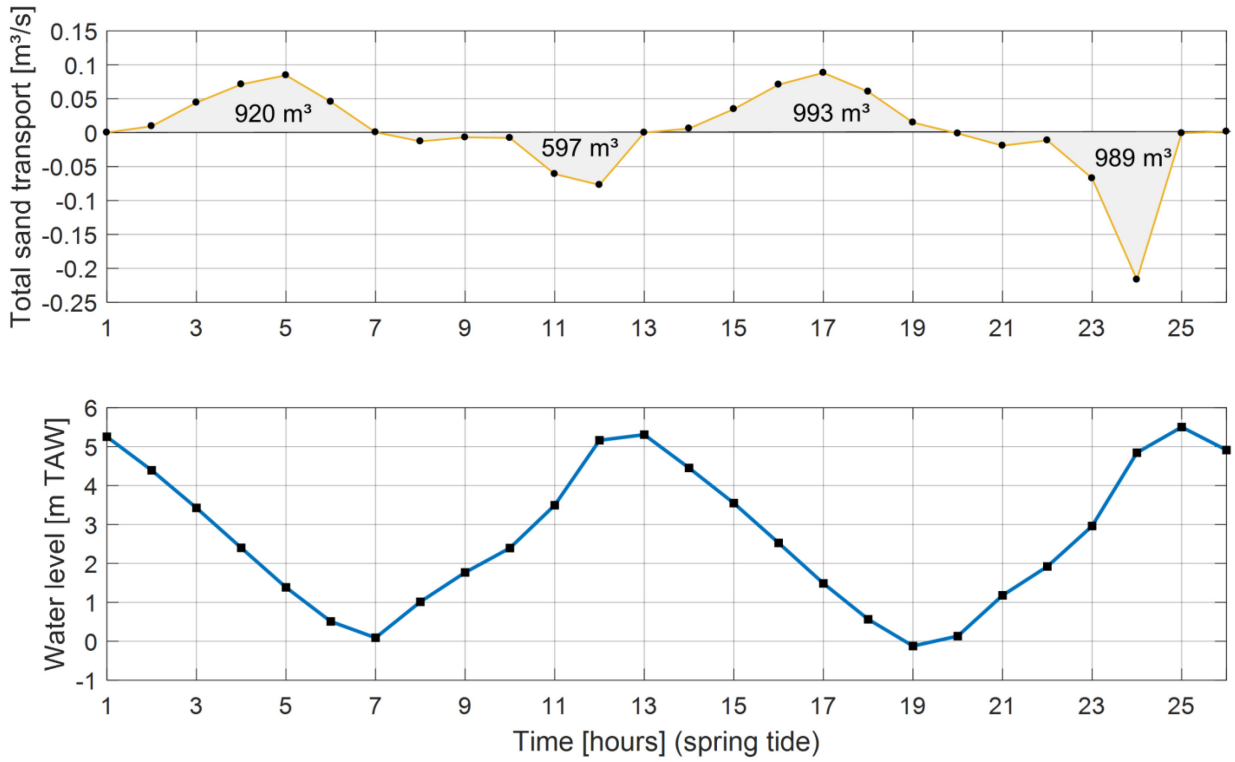

6.2 Transport equation

In the literature review in chapter 2 of this report two transport equations appear to be used frequently in estuarine models: the Engelund and Hansen equation and the Van Rijn equations. Both equations were tested in the Scaldis model both with a D50 value of 200 µm. The Van Rijn equation is a pure bed load transport equation whereas the Engelund and Hansen equation accounts for total load transport. This should result in lower transport values with the Van Rijn equation and indeed Figure 18 and Figure 19 show lower transport rates for the Van Rijn equation. Figure 18 shows however that the transport rates are lower, but the transport directions remain the same.

Figure 18 – Effect of choice of transport equation on net sand transport over different transects along the Scheldt estuary.
A positive net transport is transport in the downstream direction. A negative net transport is transport in the upstream direction.

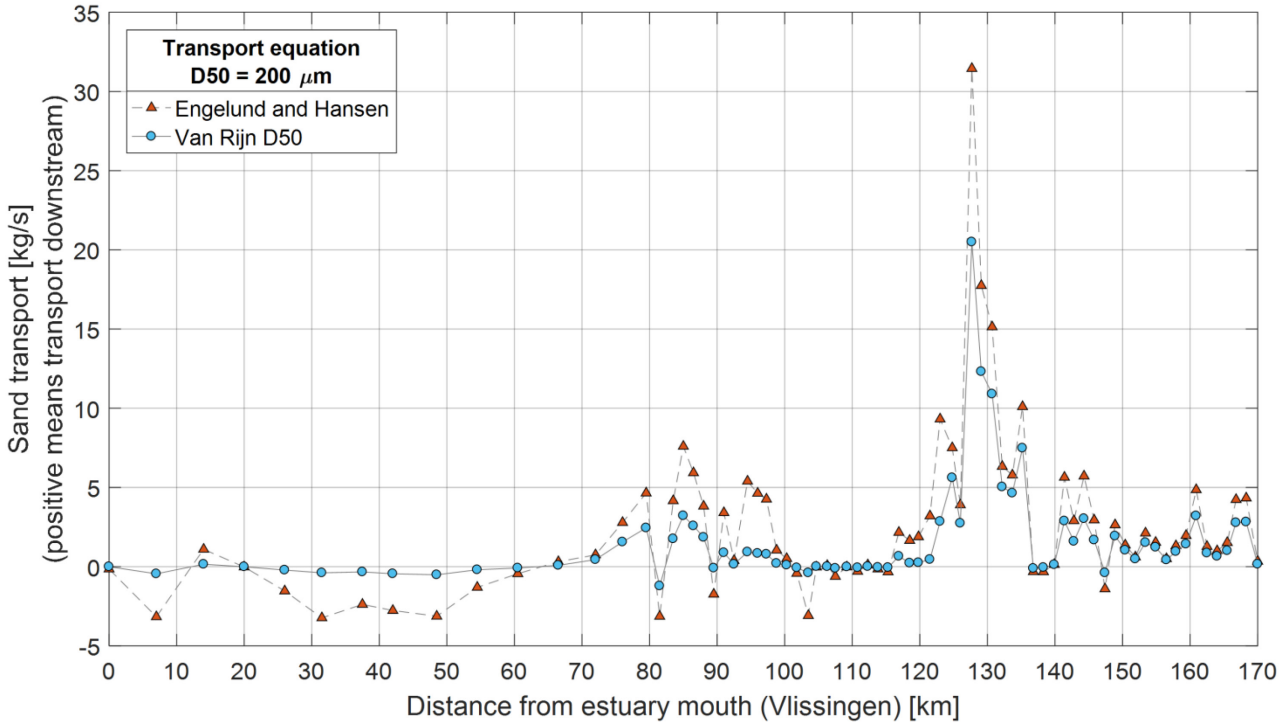

Figure 19 – Time series of sand transport over transect 23 at 92 km from the estuary mouth at Vlissingen
for different transport equations.
A positive value means downstream transport and a negative value means an upstream transport.

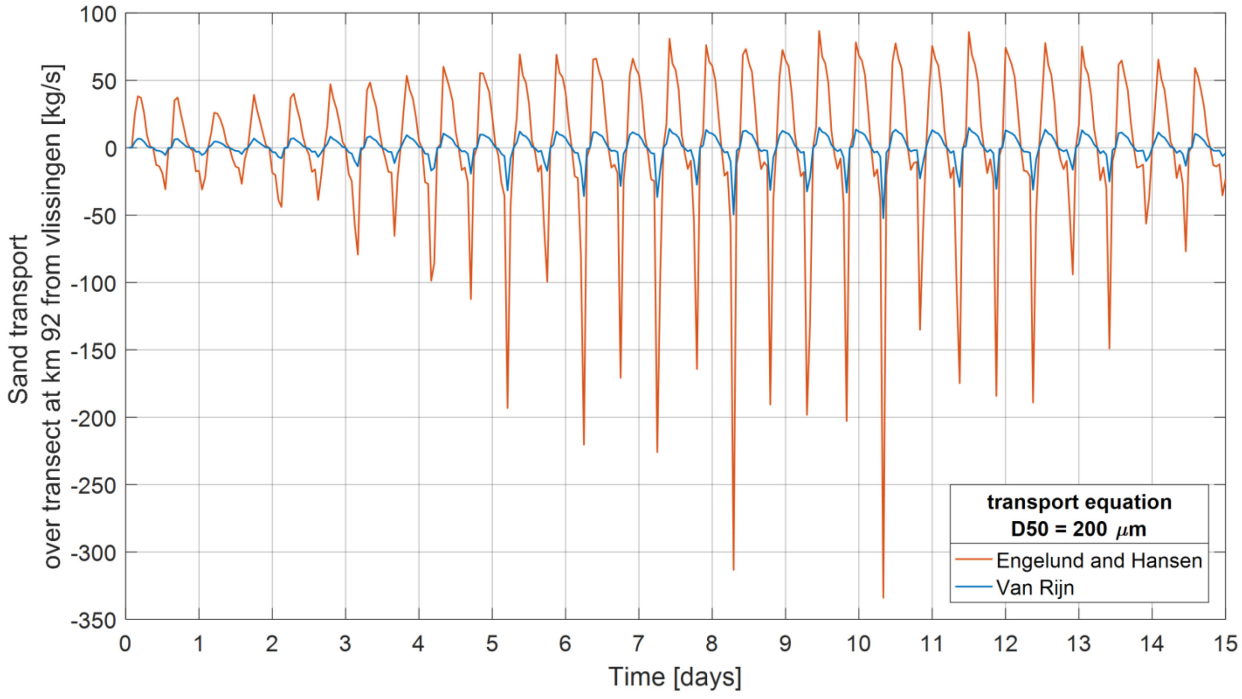

6.3 Slope effect

The slope effect makes the sediment transport go not only in the flow direction but also partly in the direction of the slope. This effect is by default taken into account. To have an idea about the magnitude of this effect on net transport rates over transects along the Scheldt estuary, a simulation without slope effects was done and showed minor differences in transport rates mainly for the Upper Sea Scheldt (where the channel is narrow and slopes are more dominant) (Figure 20).

Figure 20 – Effect of the slope effect on net sand transport over different transects along the Scheldt estuary.
A positive net transport is transport in the downstream direction. A negative net transport is transport in the upstream direction.

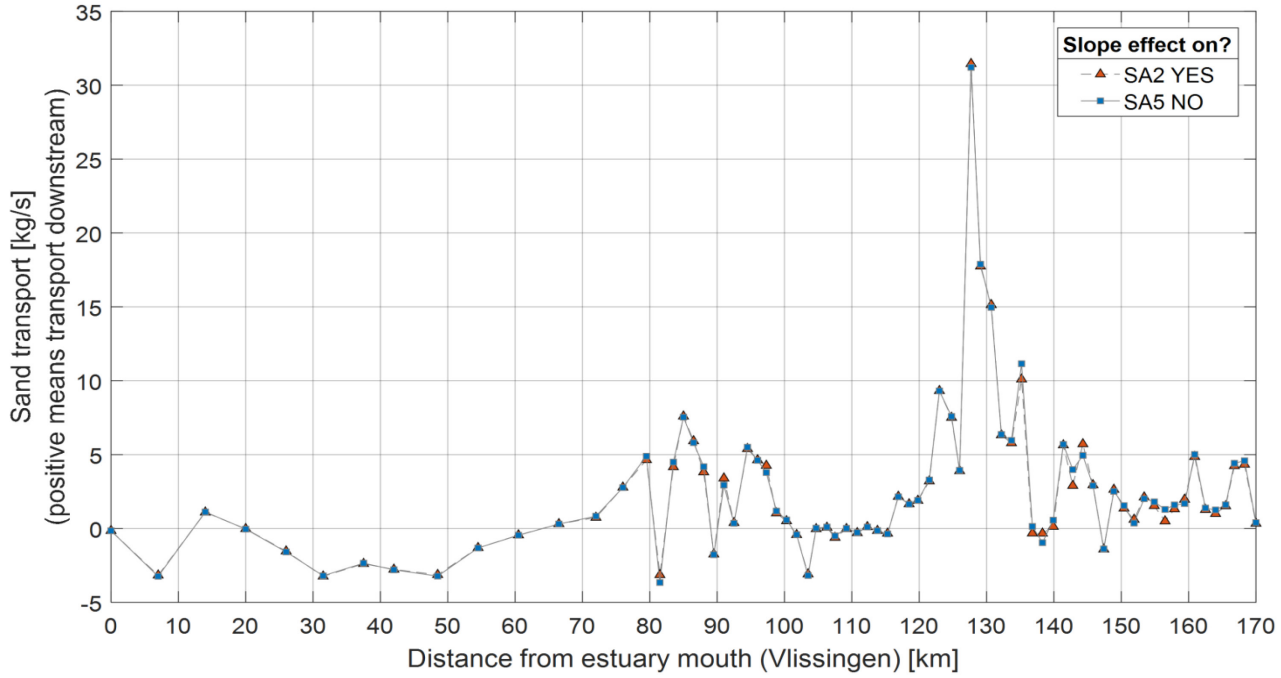

6.4 Constant Manning coefficient or spatially varying Manning from hydrodynamic simulation?

The spatial varying Manning coefficient from the hydrodynamic model is the result of a calibration exercise. This coefficient takes also no-physical processes, like numerical diffusion, into account, and therefore it is better to use a constant Manning bottom roughness coefficient for the sediment module SISPYPHE. According to equations 5.11 and 5.12, the larger the Manning coefficient, the larger the calculated bed shear stress will be. So the locations in the model domain where the constant Manning coefficient of 0.02 $m/s^{1/3}$ is larger than the coefficient given in the hydrodynamic module, will have larger sand transport rates and vice versa. This is shown in Figure 21 where the Manning coefficient in the hydrodynamic model is lower than the constant value given for the sediment module for the region between km 70 and km 90 and upstream of km 123. The differences can be big and even result in a difference in net transport direction. This also means that choosing a different constant Manning coefficient could change the net transport magnitude and direction.

Figure 22 shows the time series of sand transport over transect number 23 at km 92 along the estuary (Antwerp region) where the Manning coefficient in the hydrodynamic model is 0.021 $m/s^{1/3}$ compared to the 0.020 $m/s^{1/3}$ constant value used, resulting in higher sand transport rates over this transect for the simulation where the Manning coefficient of the hydrodynamic model was used.

Figure 21 – Effect of choice of Manning coefficient on net sand transport over different transects along the Scheldt estuary.
A positive net transport is transport in the downstream direction. A negative net transport is transport in the upstream direction.

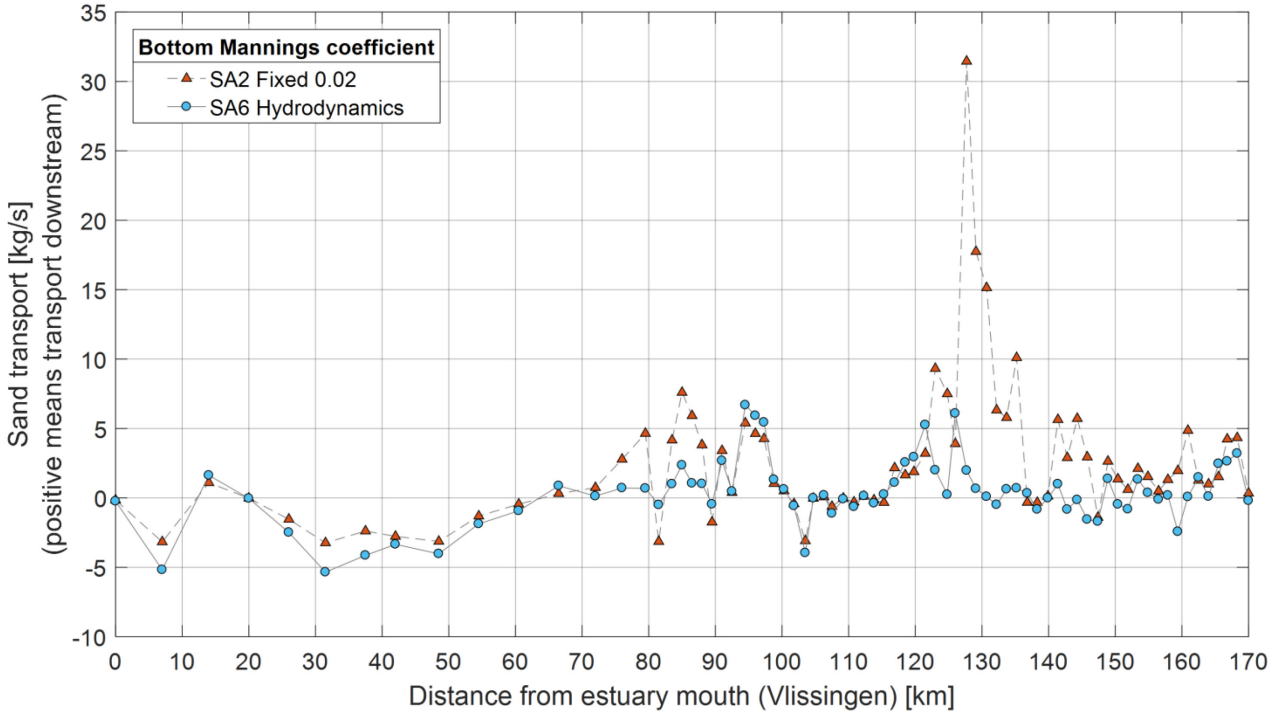

Figure 22 – Time series of sand transport over transect 23 at 92 km from the estuary mouth at Vlissingen
for different choices of the Manning coefficient.
A positive value means downstream transport and a negative value means an upstream transport.

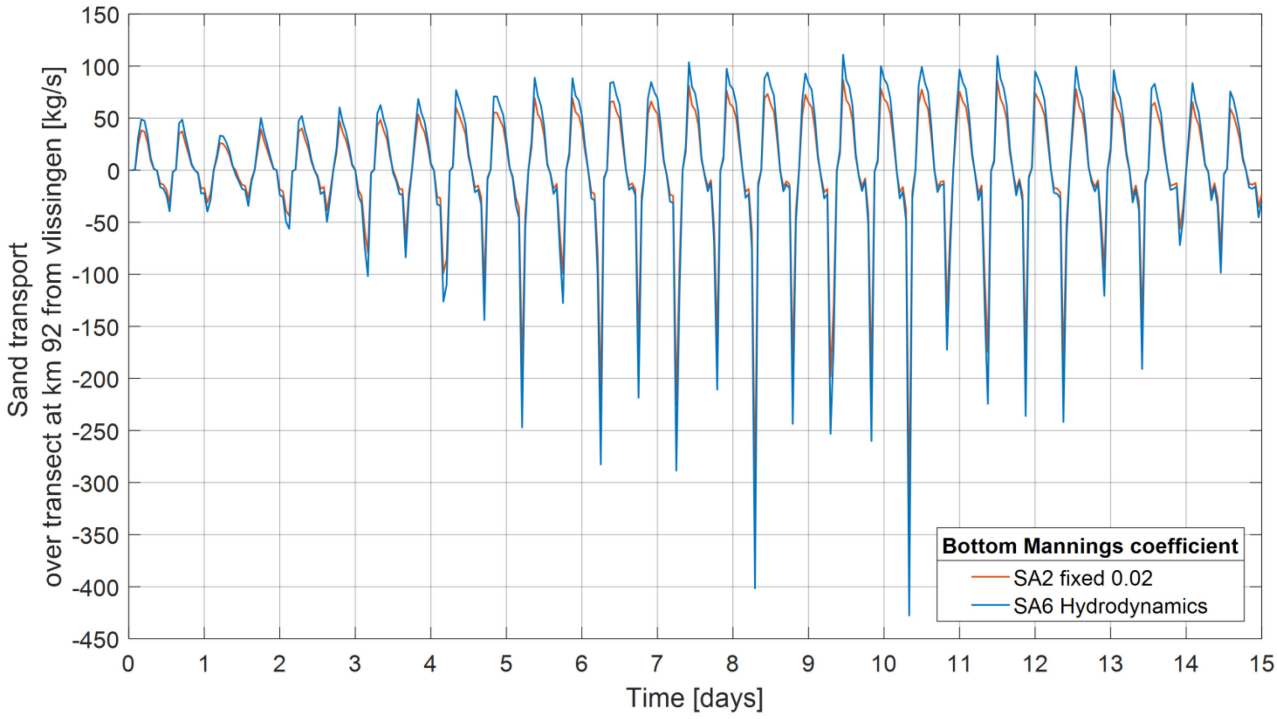

7 Model results

A simulation of 15 days with TELEMAC-3D coupled with SISYPHE was run. The downstream boundary is a forced water level combined with X and Y velocity components. The first 15 days of a synthetic QN boundary condition time series were used. QN stands for normal discharge scenario. A 15 day simulations makes sure a complete spring-neap tidal cycle is simulated. Further information about this synthetic QN boundary condition can be found in Smolders et al. (2017). The upstream boundaries (8) have a constant discharge imposed. This is 23, 34.7, 11.1, 15.92,34.6, 8.3, 10.4, 35, 0 m^3/s for the Terneuzen, Merelbeke, Dender, Zenne, Dijle, Grote Nete, Kleine Nete and Bath discharge boundary respectively. The bathymetry of 2013 is used (Smolders et al., 2016), no amplitude corrections were made (A0) and no climate sea level rise was imposed (CN). This reference run will get the name 2013_REF_QN_A0CN.

The model results will be compared with measurements (point measurements) and with estimated transport rates for different cells in the Sea Scheldt. Finally some model results of net sand transport over different transects along the Scheldt estuary will be given together with some explanation for the direction (down- or upstream) of the net transport. Combining this information over all transects results in a mass balance of the sand transport in the Scheldt estuary.

7.1 Model vs. measurements

From the 15 day simulation a tide was chosen that came closest to the tide during the 13 hour measurement campaign at the different locations. The sand transport rate close to the location of the point measurement (and taking flow velocity and water depth into account) was extracted from the model and plotted together with the measured values for total sand transport. Time in the x-axis is expressed relative to low water. The results are discussed for the different locations going from downstream to upstream.

The model is able to reproduce the results for Oosterweel very well (Figure 23), with a good peak in flood flow transport and a low base transport during ebb.

For Kruibeke (Figure 24) the measurements show a larger ebb peak in transport than during flood. The model was able to reproduce both peaks, but the maximum in the flood peak in the model is slightly higher than the ebb peak. At the beginning of flood there is a small peak of sand transport measured and the model was also able to reproduce this small peak.

The measured sediment transport in Driegoten (Figure 25) contained a large fraction of mud. The calculated total sand transport shows no clear trend. The model however shows a clear broad peak during ebb and a small peak during flood. The comparison is difficult and shows no good overlap of both results, but the order of magnitude of both model and measured total transport is the same.

The model results and measured transport rates at Dendermonde are in very good agreement with each other (Figure 26). The sand transport rates during ebb flow are a little overestimated by the model, but the flood peak is very well reproduced.

For Schoonaarde (Figure 27) the measured sand transport is very low. The order of magnitude is reproduced by the model, but the model overestimates the transport during the flood peak.

Like at Schoonaarde the measured sand transport rate at Schellebelle (Figure 28) is very low, but the model is able to reproduce this transport rates very well, both during ebb and flood.

For Terhagen on the Rupel (Figure 29) the model is able to reproduce the ebb peak reasonable, but overestimates the flood peak. In the measurements there is almost no peak in sand transport during flood. The model shows a clear peak during flood.

Figure 23 – Oosterweel sand transport rate: model result vs. measurements

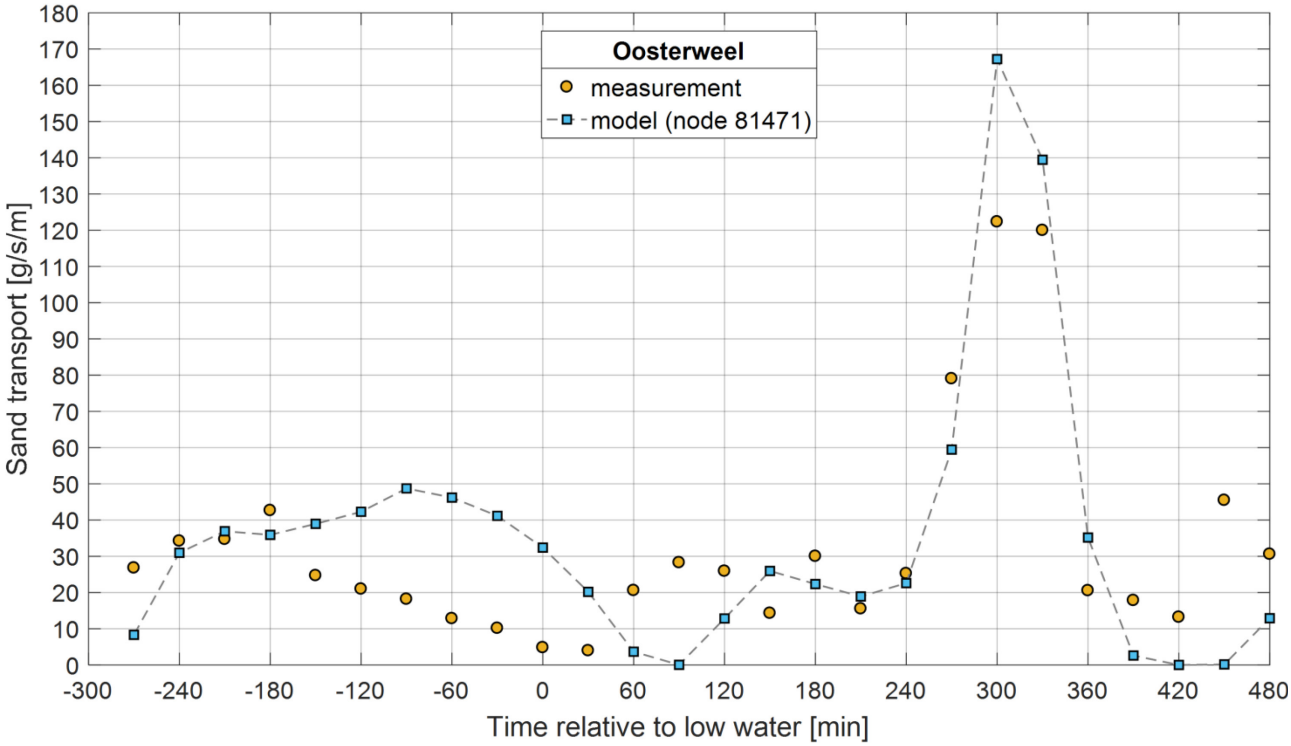

Figure 24 – Kruibeke sand transport rate: model result vs. measurements

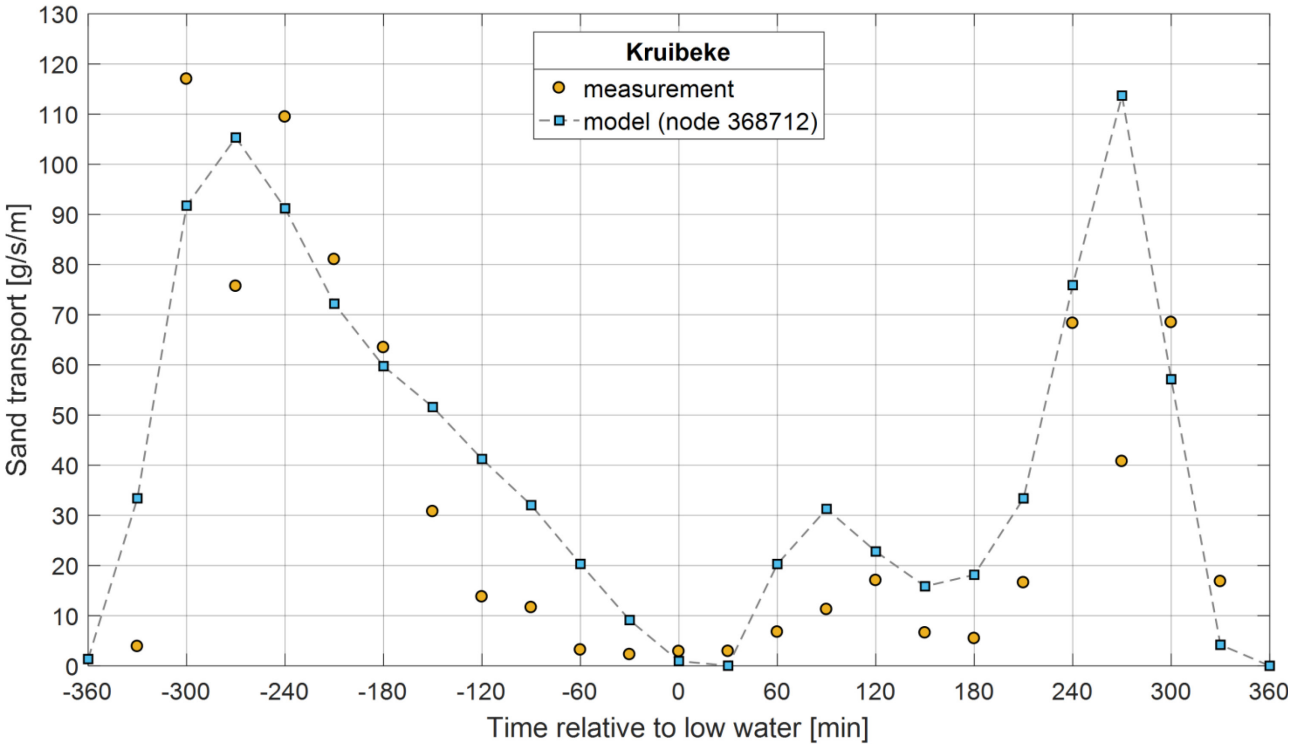

Figure 25 – Driegoten sand transport rate: model result vs. measurements

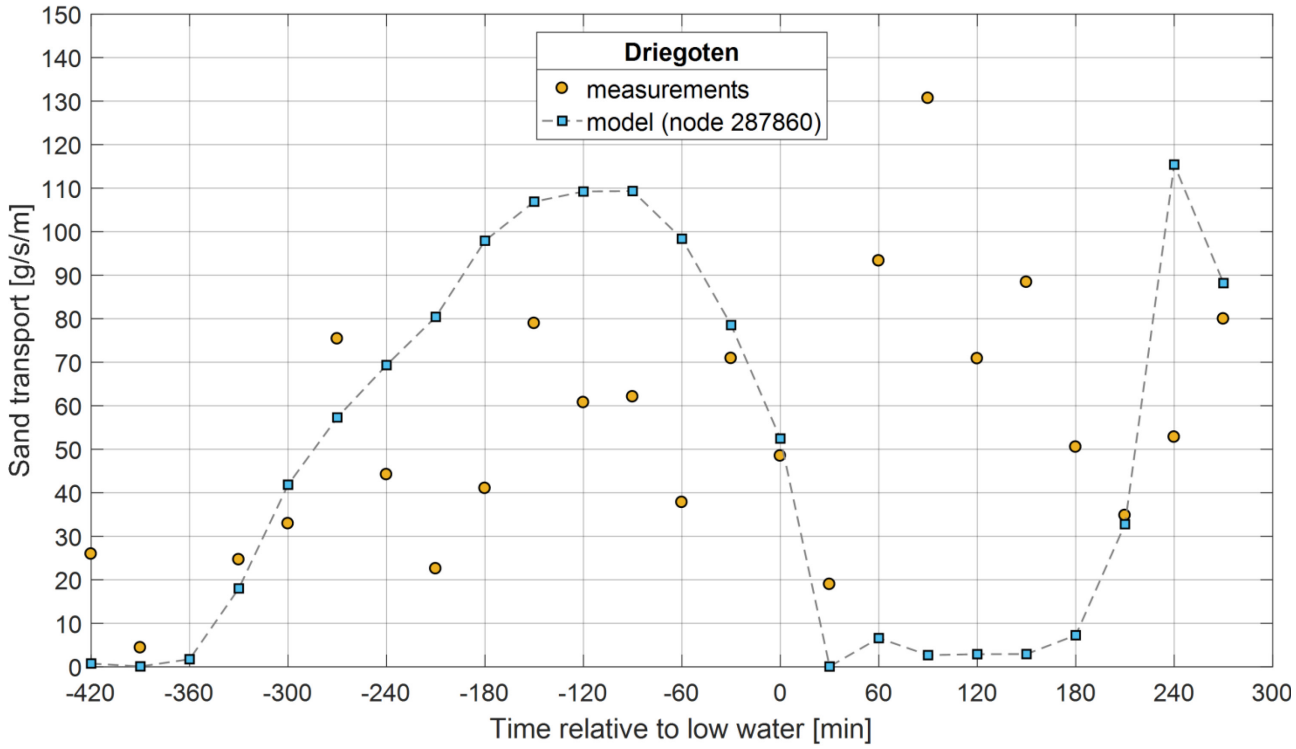

Figure 26 – Dendermonde sand transport rate: model result vs. measurements

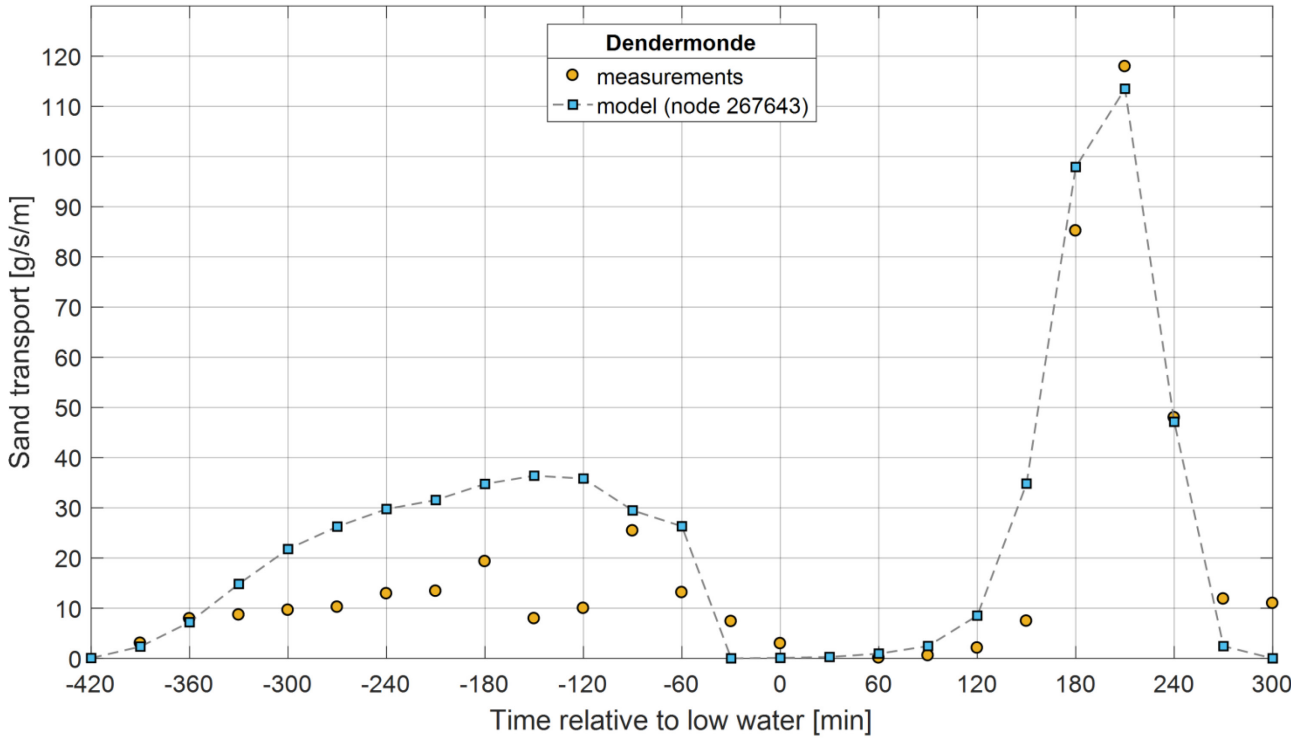

Figure 27 – Schoonaarde sand transport rate: model result vs. measurements

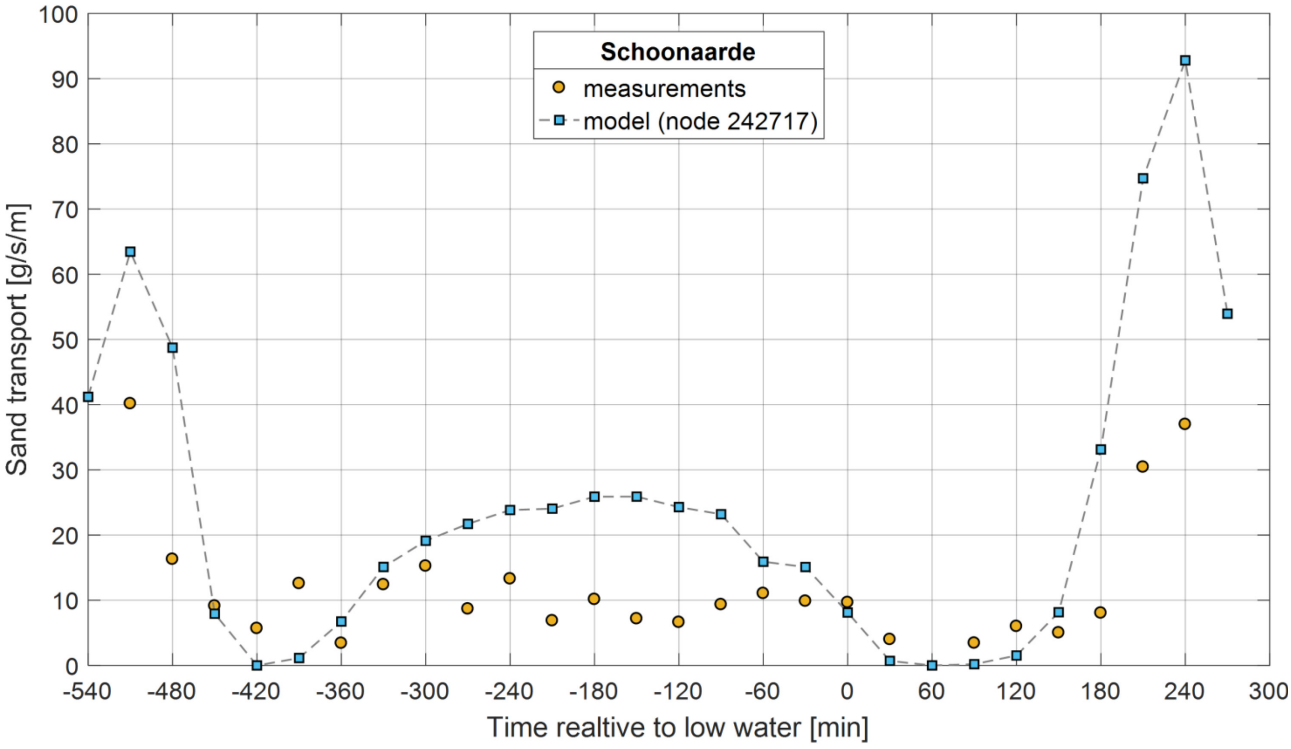

Figure 28 – Schellebelle sand transport rate: model result vs. measurements

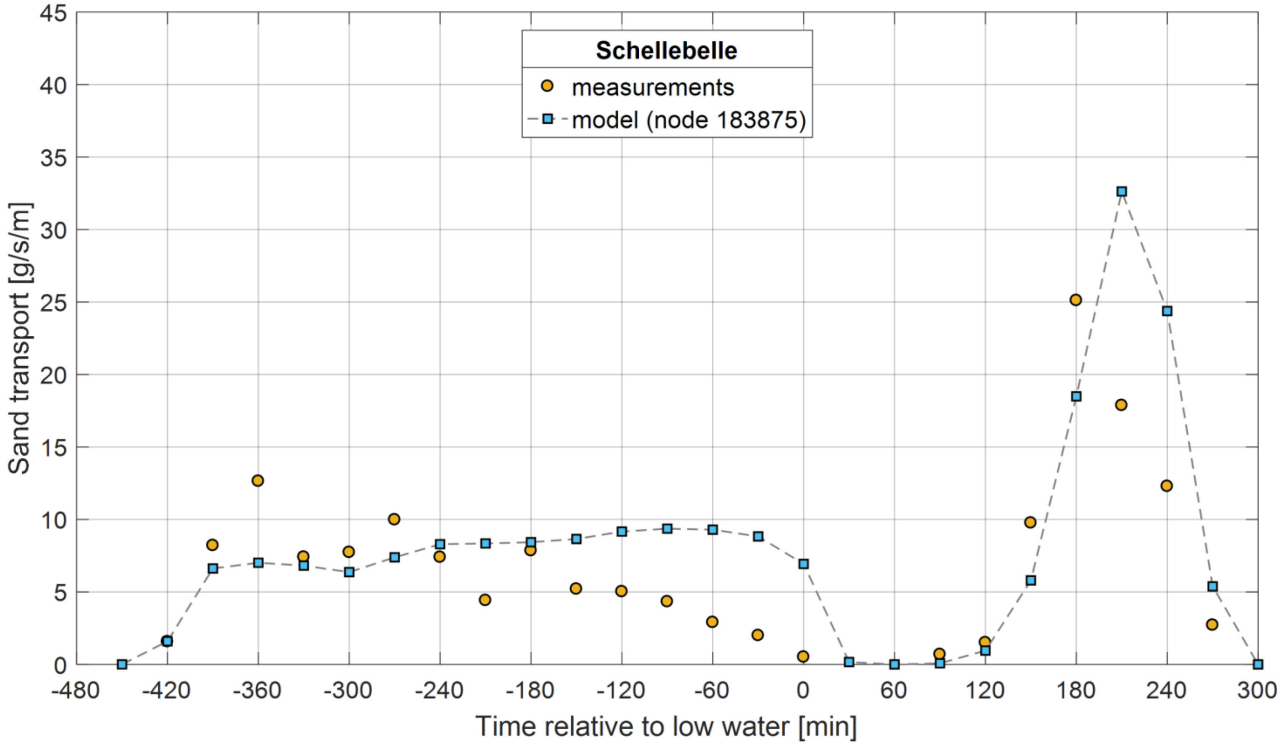

Figure 29 – Terhagen sand transport rate: model result vs. measurements

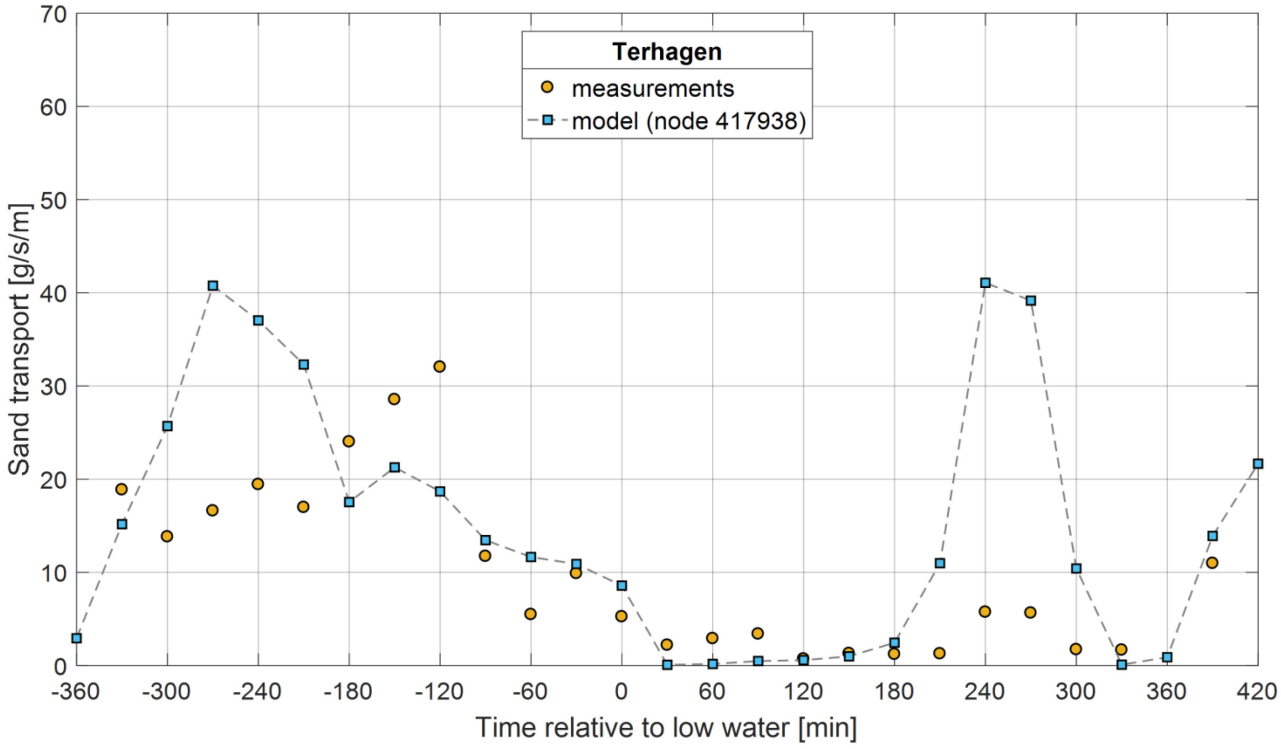

7.2 Model vs. calculated 10 yearly sand transport and transport directions

Model results and calculated transport number over the OMES boxes are shown in Figure 30. The model results are scaled up from a net transport over a spring-neap tidal cycle (15 days) to a net transport over a period of 1 year. The calculated sand transport from Vandenbruwaene et al. (2017) is scaled down from a transport over ten years to a transport number of one year and was then adjusted to take a bed porosity of 0.5 into account. For the Upper Sea Scheldt the model shows a very good agreement with the calculated sand transport, both in magnitude as in transport direction. The model tends to underestimate the sand transport a little, mainly in the lower Sea Scheldt. For the tidal arm to Gentbrugge (OMES box 19 in Figure 30), the model gives a net import, although very small, and the calculated sand transport gives a value 200 times larger. In the sand transport model the Durme is importing sand like the calculated transport. The value given by the model is much smaller than the calculated import. For the Lower Sea Scheldt the model results give mainly ebb dominated sand transport, whereas the calculated transports are directed upstream. Transport rates are in the same order of magnitude, except for the three transects closest to the border; there the model results are much smaller than the calculated results. Larger scale changes to the estuary like dredging and dumping and de-embankments are not included in a short model run, but it is unclear if this might give the difference seen in the sand transport numbers and directions in the Lower Sea Scheldt. In Coen et al. (2018) a sand transport model is used for the Scheldt estuary and on the Dutch/Belgian border the transport directions show also a net downstream transport direction.

Figure 30 – Sand transport over OMES boxes. Model results versus calculated sand transport.

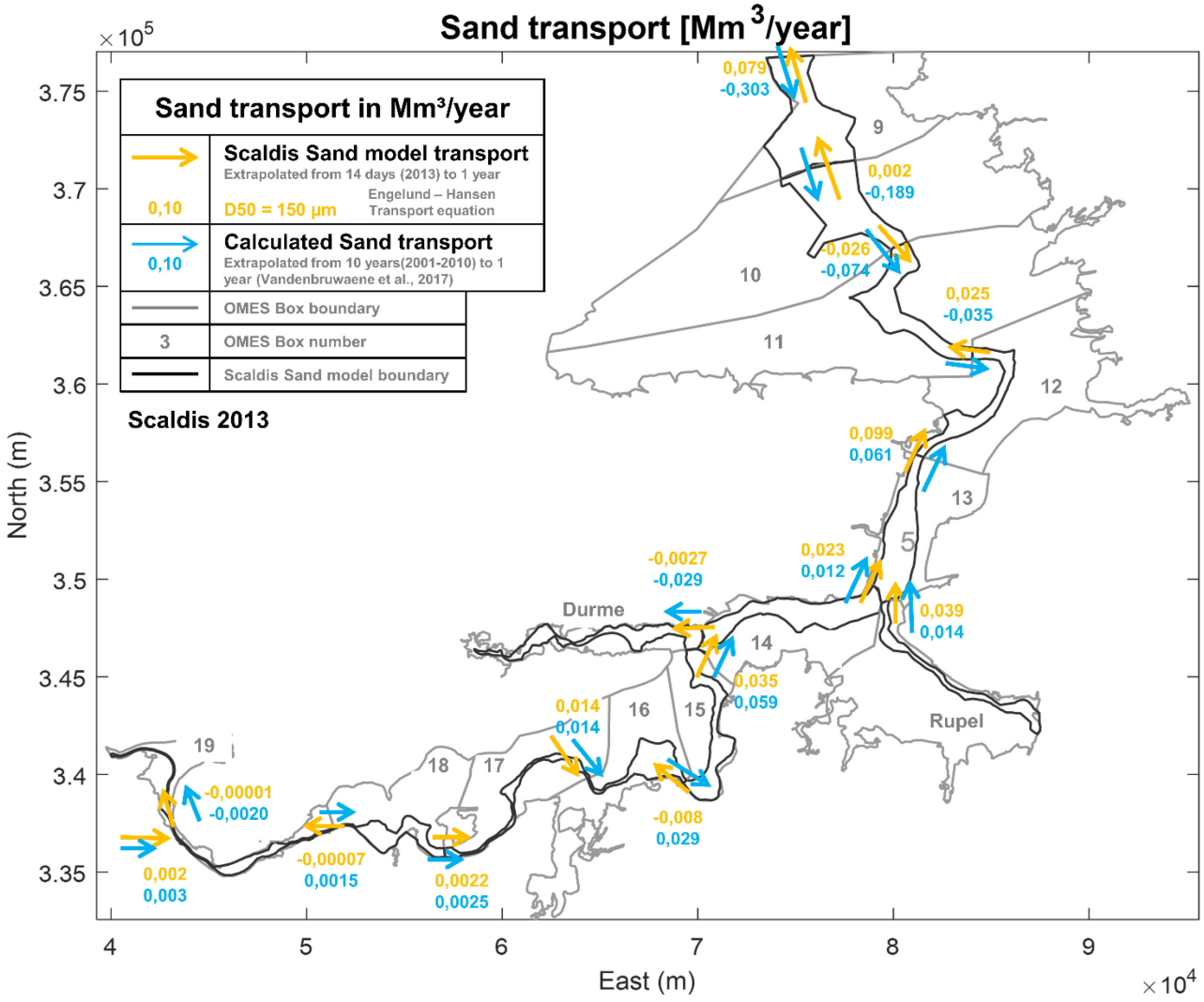

7.3 Sand transport over transects along the estuary

The net sand transport over transects can be calculated for different type of tides: neap and spring tide or averaged over a spring/neap tidal cycle tide (Figure 31).

Figure 31 shows that for an averaged spring/neap tidal cycle the sand transport in the Western Scheldt is directed upstream (negative value). Around the Dutch-Belgian border the direction of the transport changes to downstream. The sand transport increases a lot between km 90 and 100 in downstream direction with some peaks with upstream transport in between. In the Upper Sea Scheldt the transport direction is usually downstream with one exception around km 147 (around Schoonaarde). The transport rate during a neap or spring tide behave differently and are also plotted in Figure 31. In most cross sections the transport rate increase during spring tide and decreases during neap tide, but in the Upper Sea Scheldt starting from km 132 the opposite trend is seen (Figure 32). Around km 130 there are a series of sharp bends (Kramp) in the estuary. Sometimes the net transport direction changes when going from a neap tide to a spring tide, like around km 100-115 (Figure 32).

Figure 31 – Net sand transport over different cross sections along the Scheldt estuary calculated and plotted for a neap and spring tide, and averaged over a spring/neap tidal cycle. A positive value means transport in downstream direction.

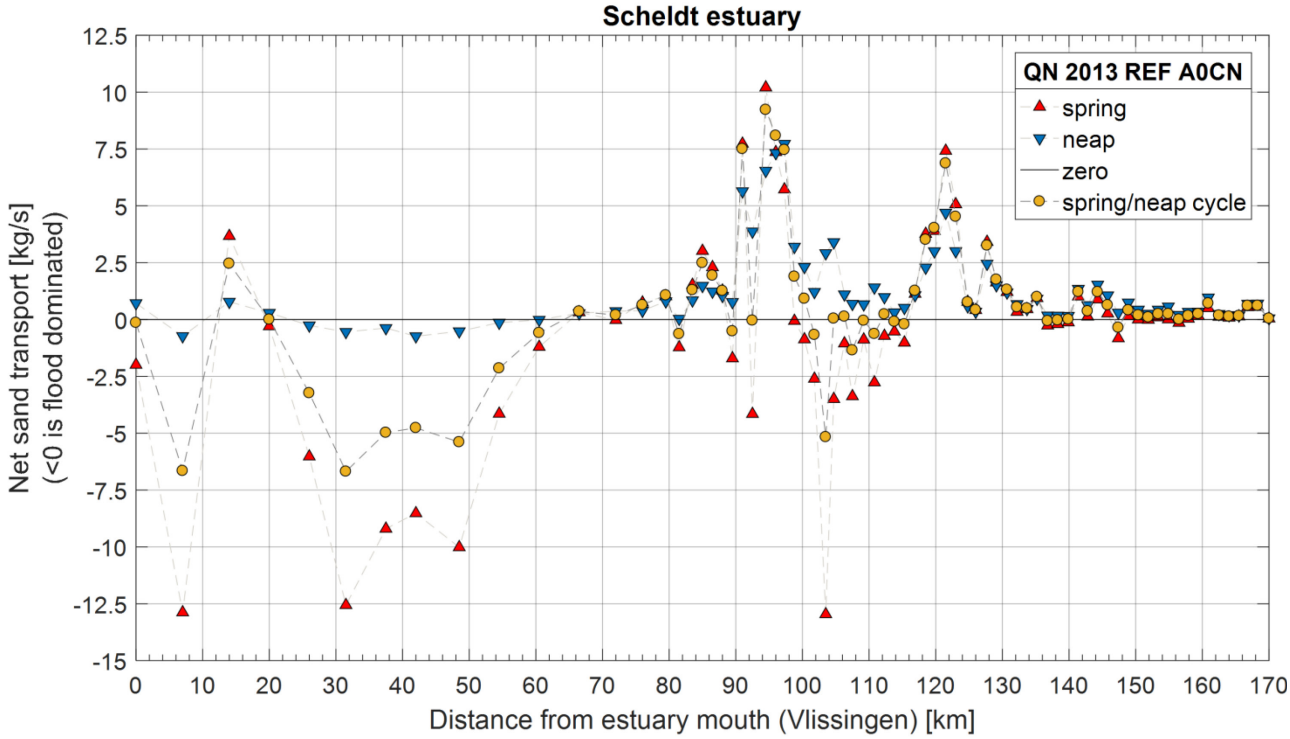

Figure 32 – Net sand transport over different cross sections along the Upper Sea Scheldt calculated and plotted for a neap and spring tide, and averaged over a spring/neap tidal cycle. A positive value means transport in downstream direction.

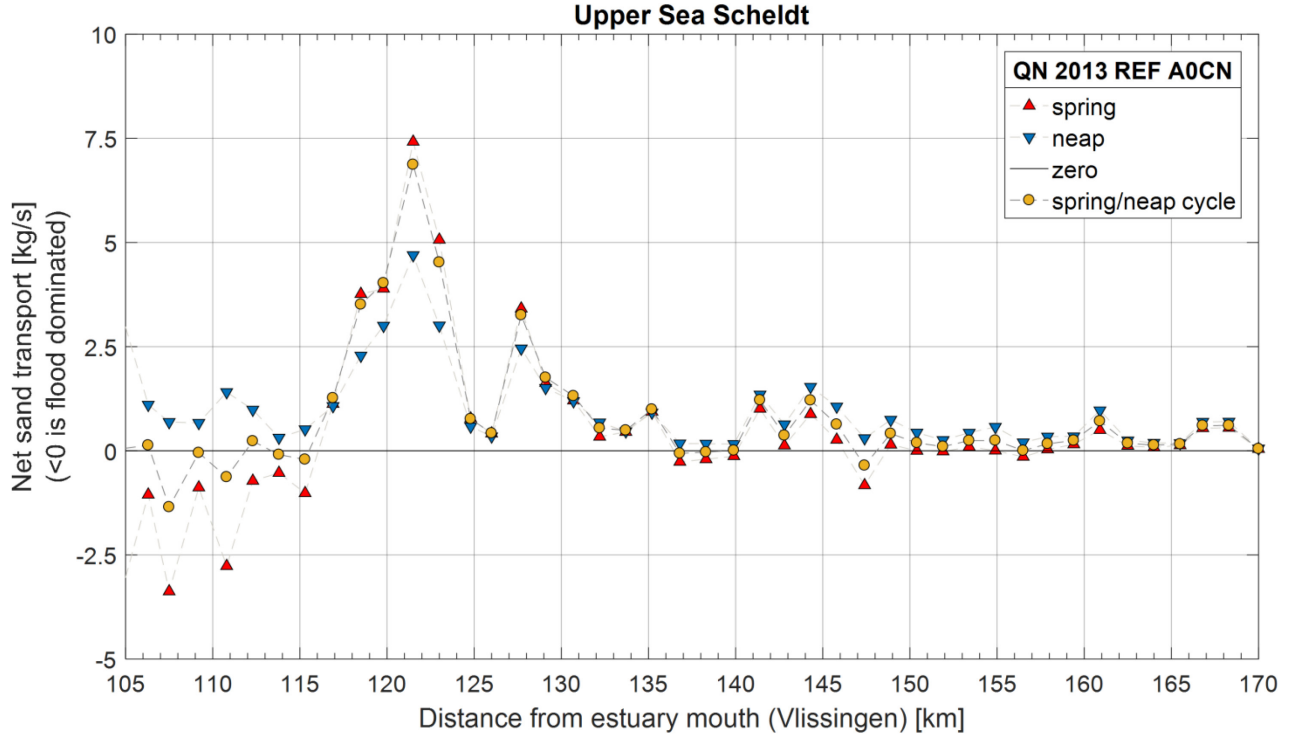

Since the flow velocity to the power five is the largest driving force behind the Engelund and Hansen equation (equation 5.6) and since there is no threshold for this velocity for incipient motion, an integration of both flood and ebb cross sectional averaged flow velocity to the power five can give more insight in why the net sand transport is going in up- or downstream direction. The asymmetry between the integrated cross sectional averaged flood and ebb velocity to the power five is shown in Figure 33. The asymmetry is shown for an integration over a full spring-neap tidal cycle and for an integration over two spring (diurnal inequality) and two neap tides separately. When the asymmetry is larger than 1 it means that the flow velocity to the power five is larger in the upstream direction and is thus flood dominated. If the asymmetry is smaller than 1 it is ebb dominated. Since cross sectional averaged flow velocities are used, the spatial variation along the transect is lost. Figure 33 shows that for the Western Scheldt the asymmetry is mostly larger than 1, which coincides with the upstream direction of the transport found in Figure 31 and Figure 32. Around the Dutch-Belgian border (km 65) the asymmetry drops below 1, changing the direction of the transport to downstream. Between km 100 and 115 the transport direction changed again from downstream to upstream and this also shows in Figure 40 where the asymmetry rises again above 1. In the Upper Sea Scheldt the asymmetry is mostly below 1 and the transport direction is ebb dominated. One peak in asymmetry above 1 can be seen around km 138 and this coincides with a reduced transport in the ebb direction, but the net sand transport doesn't change entirely to the upstream direction. The spring and neap tide markers show that asymmetry can change a lot between these two extreme in tides and can also change the dominance from ebb to flood or vice versa.

Figure 33 – Asymmetry between flood and ebb over time integrated cross sectional averaged flow velocity to the power five.

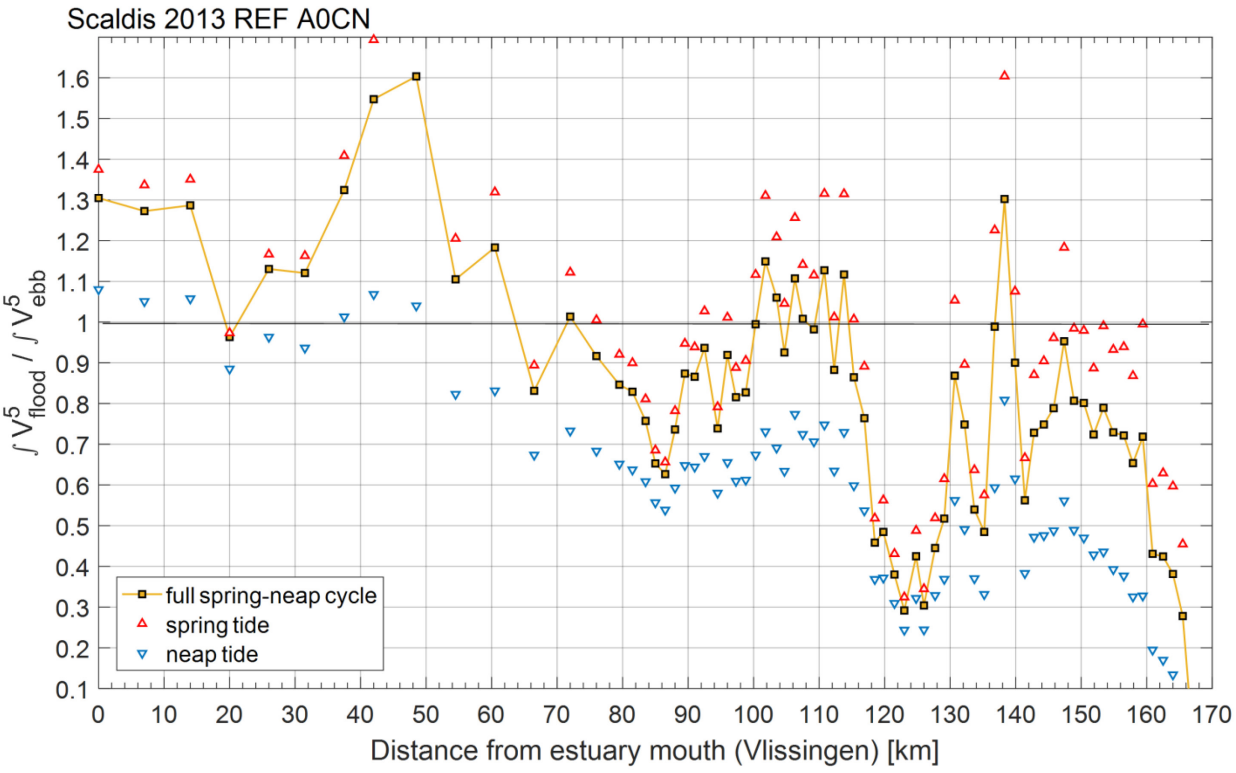

7.4 Mass balance

The sand transport over the different transects along the Scheldt estuary was calculated for a full spring-neap tidal cycle. The polygons formed in between the transect are used to calculate a mass balance. This sand mass balance is shown in Figure 34. This figure shows the areas in the Upper Sea Scheldt that are accumulating sand (in red colors) and other areas that are eroding and thus losing sand (in blue colors). The net accumulation or erosion of a polygon in the Upper Sea Scheldt area extrapolated to one year is listed in Table 3 in Appendix C.

Figure 34 – A sand mass balance calculated after a full spring-neap tidal cycle and extrapolated to one year based on calculated transports over transects for run QN 2013 REF A0CN.

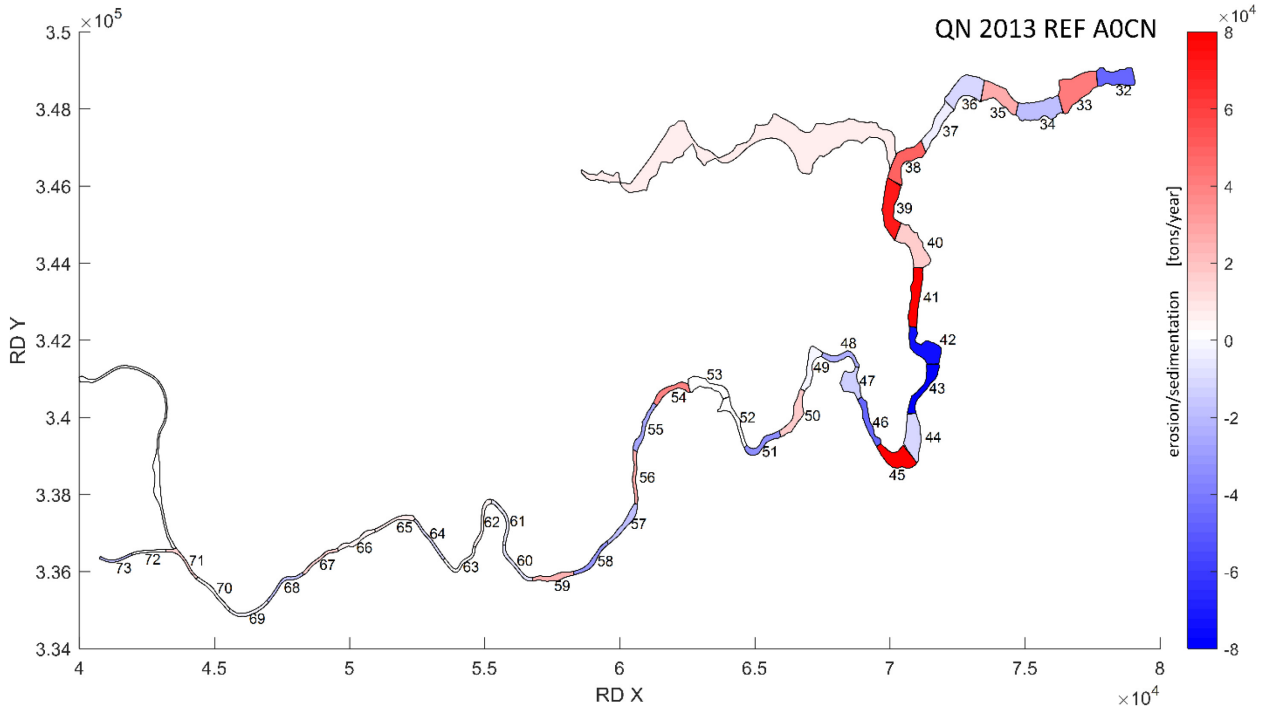

8 Conclusions

This report describes a sand transport model for the Scheldt estuary. It starts with describing the extensive work that has been done in previous projects on this topic in a literature review. Based on this experience parameter settings were chosen for the sand transport model. A single fraction of sand is used over the entire model domain. The D50 grain size value was chosen close to an average value obtained by a measurement campaign in 2014 (=130 µm, Plancke et al., 2014), i.e. 150 µm. The Engelund and Hansen total load equation was chosen as transport equation. The hydrodynamic data was delivered by the 3D Scaldis model. The bottom of this model was not updated during the simulation period of 15 days (a full spring-neap tidal cycle). The bottom evolution and mass balance was only tracked with the sediment transport module, SISYPHE. The sediment module used a constant Manning bottom friction coefficient of 0.020 $m/s^{1/3}$.

A sensitivity analysis shows that an increase in grain size, decreases the net sand transport. It further showed that the larger the bottom friction coefficient is chosen, the larger the bottom shear stress becomes and the larger the sand transport becomes. There is also a large difference in sand transport when switching from the Engelund and Hansen equation to the Van Rijn equation in default settings. The Engelund and Hansen equation, being a total load equation, predicts larger transport rate than the Van Rijn equation.

When the model results are compared to point measurements for total sand transport most locations show a very good agreement, like Oosterweel, Kruibeke, Dendermonde and Schellebelle, while at other locations the model overestimated the transport rate during the flood peak, like Schoonaarde and Terhagen. At Driegoten the measured total sand transport doesn't show a clear trend, whereas the model has a clear broad peak during ebb and a narrow peak during flood.

Comparing model results with calculated net sand transport rates based on the difference of bathymetry measurements between 2001 and 2010 showed that the model reproduces the sand transport rate and directions in the Upper Sea Scheldt well, but underestimates the transport rate in the Lower Sea Scheldt and finds opposite directions of transport close to the Dutch/Belgian border.

Finally transport rates over transects are shown for the entire estuary and most of the transport rates and directions can be explained by the integration over time of the cross sectional averaged flow velocity to the power five (as it is used in the Engelund and Hansen equation).

9 References

Chollet J.P. and Cunge J.A. (1979). New interpretation of some head loss-flow velocity relationships for deformable movable beds. Journal of Hydraulic Research, vol. 17, no. 1, pp. 1—13.

Coen, L.; Plancke, Y.; De Maerschalck, B.; Mostaert, F. (2018). Agenda voor de Toekomst Morfologie Mesoschaal: Deelrapport 13 – Scenario's morfologisch beheer. Versie 4.0. WL Rapporten, 14_024_13. Waterbouwkundig Laboratorium: Antwerpen.

Einstein, H.A., 1950. The Bed-Load Function for Sediment Transportation in Open Channel Flow. Technical Bulletin No. 1026, U.S. Dep. of Agriculture, Washington, D.C.

Engelund, F. and Hansen, E., 1967. A Monograph on Sediment Transport in Alluvial Streams. Teknisk Forlag, Copenhagen, Denmark.

Engelund, F., 1974. Flow and bed topography in channel bends. Journal of the Hydraulics Division 100 (HY11), 1631–1648.

Flokstra, C.; Koch, F. (1981). Numerical aspects of bed level predictions for alluvial river bends. Delft Hydraulics Laboratory. Netherlands, Publication 258

Huisman, B. J. A., Ruessink, B. G., De Schipper, M. A., Luijendijk, A. P., & Stive, M. J. F. (2018). Modelling of bed sediment composition changes at the lower shoreface of the Sand Motor. *Coastal Engineering*, *132*, 33-49.

Koch, F.G., Flokstra, C., 1981. Bed level computations for curved alluvial channels, In: Proceedings of the Nineteenth Congress of the International Association for Hydraulic Research, New Delhi, India, pp. 357–364.

Kolokythas, G.; Wang, L.; Fonias, S.; De Maerschalck, B.; Vanlede, J.; Mostaert, F. (2018). Modelling Belgian Coastal zone and Scheldt mouth area: Sub report 6: Progress report 2- Evaluation of numerical modelling tools and model developments. Version 5.0. FHR Reports, 15_068_65. Flanders Hydraulics Research: Antwerp.

Maximova, T.; Vanlede, J.; Plancke, Y.; Verwaest, T.; Mostaert, F. (2013). Habitatmapping ondiep water Zeeschelde: deelrapport 2 - Numeriek 2D model. Version 2.0. WL Rapporten, 00_028. Waterbouwkundig Laboratorium: Antwerp. IX, 60 + 87 p. appendices pp.

Mendoza A., Abad J.D., Langendoen E., Wang D., Tassi P., and El Kadi Abderrezzak K. Effect of sediment transport boundary conditions on the numerical modeling of bed morphodynamics. J. of Hydr. Eng., 2016.

Meyer-Peter, E. and Mueller, R., 1948. Formulas for Bed-Load Transport. Sec. Int. IAHR congress, Stockholm, Sweden.

Nnafie, A.; Van Oyen, T.; De Maerschalck, B. (2015). Telemac2D and Delft3D morphodynamic models: A model comparison. Concept Version. WL Memo, 14_094_5. Waterbouwkundig Laboratorium: Antwerpen

Plancke, Y.; Vereecken, H.; Vanlede, J.; Verwaest, T.; Mostaert, F. (2014). Integraal plan Boven-Zeeschelde: Deelrapport 3 – Factual data-rapport sediment transport metingen in de Zeeschelde in 2014. Versie 4.0. Wl Rapporten, 13_131. Waterbouwkundig Laboratorium: Antwerpen, België.

Plancke, Y.; Smolders, S.; Mostaert, F. (2018). Sedimenttransport in het Schelde-estuarium: Deelrapport 1 – Bepalen van het aandeel zandtransport uit metingen met de Delftse fles. Versie 1.0. WL Rapporten, 16_001_1. Waterbouwkundig Laboratorium: Antwerpen.

Ridderinkhof, W.; Swart, H. E. de; Vegt, M. van der; Hoekstra, P. (2014). Influence of the backbarrier basin length on the geometry of ebb-tidal deltas. Ocean Dynamics 64, pp. 1333–1348. DOI: 10.1007/s10236-014-0744-3.

Robins, P. E., & Davies, A. G. (2010). Morphodynamic processes in shallow estuaries: influence of tidal flats and channels on sand transport. *Ocean Dynamics*, *60*, 503-517.

Schramkowski, G.P.; Luyten, P.; Heredia Gomez, M.; Rauwoens, P.; Van Oyen, T.; Monbaliu, J.; Komijani, H; Breugem, A.; Delecluyse, K; Chu, K.; Lee, B.J; Verwaest, T.; Mostaert, F. (2016). COHERENS validation report. Version 1.0. FHR reports, 00_147_1. Flanders Hydraulics Research: Antwerp.

Smolders, S.; Maximova, T.; Vanlede, J.; Plancke, Y.; Verwaest, T.; Mostaert, F. (2016). Integraal Plan Bovenzeeschelde: Subreport 1 – SCALDIS: a 3D Hydrodynamic Model for the Scheldt Estuary. Version 5.0. WL Rapporten, 13_131. Flanders Hydraulics Research: Antwerp, Belgium.

Smolders, S.; Maximova, T.; Vandenbruwaene, W.; Coen, L.; Vanlede, J.; Verwaest, T.; Mostaert, F. (2017). Integraal Plan Bovenzeeschelde: Deelrapport 5 – Scaldis 2050. Version 4.0. FHR Reports, 13_131_5. Flanders Hydraulics Research: Antwerp.

Soulsby, R.L. 1997. Dynamics of Marine Sands: a Manual for Practical Applications. Telford, London, p. 249.

Talmon, A.M., 1992. Bed topography of river bends with suspended sediment transport. Communications on hydraulic and geotechnical engineering. Report 92-5. TU Delft.

Talmon, A.M.; Struiksma, N.; and van Mierlo, M.C.L.M. Laboratory measurements of the direction of sediment transport on transverse alluvial-bed slopes. J. of Hydr. Res., 33(4): 495–517, 1995.

Van Dam, T. (2014). Morfologie en hydrodynamica in de Beneden-Zeeschelde: Ontwikkelingen van 1960 tot 2010. Svasek Hydraulics: Rotterdam, Nederland.

Vandenbruwaene, W.; Levy, Y.; Plancke, Y.; Vanlede, J.; Verwaest, T.; Mostaert, F. (2017). Integraal plan Boven-Zeeschelde: Deelrapport 8 – Sedimentbalans Zeeschelde, Rupel en Durme. Versie 4.0. WL Rapporten, 13_131_8. Waterbouwkundig Laboratorium: Antwerpen.

Villaret, C., Hervouet, J. M., Kopmann, R., Merkel, U., & Davies, A. G. (2013). Morphodynamic modeling using the Telemac finite-element system. *Computers & Geosciences*, *53*, 105-113.

Vos, G.; De Maerschalck, B.; Plancke, Y.; Verwaest, T.; Mostaert, F. (2016). Sedimentstrategie Beneden-Zeeschelde: Deelrapport 2 – Opzet en validatie zandmodel. Versie 4.0. WL Rapporten, 14_025. Waterbouwkundig Laboratorium: Antwerpen, België.

Appendix A: list of all relevant keywords and their default values for bedload sediment transport in SISPYHE

Table 2 – Overview of keywords in SISYPHE for sand transport

Keyword	**Default value**	**Explanation**
BED LOAD	YES	*Takes bed load transport into account*
GRAVITY ACCELERATION	9.81	*Sets the value of the acceleration due to gravity [m/s²] = g*
WATER DENSITY	1000	*Sets the value for the density of water [kg/m³] =ρ*
SEDIMENT DENSITY	2650	*sets the value of the sediment density [kg/m³] = ρ_s*
BED-LOAD TRANSPORT FORMULA	1	*The formula Ne3, Ne30 and Ne9 should not be used in the case of coupling with the suspension. The formula Ne4, Ne5, Ne8 and Ne9 model the transport under the combined action of currents and waves :* *1 : MEYER-PETER (bed load)* *2 : EINSTEIN-BROWN (bed load)* *3 : ENGELUND-HANSEN + CHOLLET AND CUNGE (VERSION 5.3)* *30: ENGELUND-HANSEN (total)* *4 : BIJKER (bed load + suspension)* *5 : SOULSBY - VAN RIJN (bed load + suspension)* *6 : HUNZIKER (only for sand grading; and HIDING FACTOR keyword is discarded and the Hunziker formula is used.)* *7 : VAN RIJN (bed load)* *8 : BAILARD (bed load + suspension)* *9 : DIBAJNIA ET WATANABE (total)* *Users can also program other formulas (subroutine QSFORM.f) setting this key word to zero :* *0 : FORMULA PROGRAMMED BY USER* *Warning : it is not then possible to choose the option VARIABLE TIME-STEP*

SKIN FRICTION CORRECTION	1	*formula to predict the skin bed roughness (see also KSPRATIO)* *0 : NO correction (TAUP= TOB)* *1 : Flat bed (KSP= KSPRATIO * D50)* *2 : Ripple correction factor*
RATIO BETWEEN SKIN FRICTION AND MEAN DIAMETER	3.0	*= KSPRATIO; Ratio for the computation of skin friction. skin roughness = ratio * mean diameter (for the mixture of sand, the mean diameter used is a value per node which is computed thanks to the fraction and the mean diameter of each sediment for each node of the mesh) if KSPRATIO =0 : use skin friction prediction from Van Rijn (2007) for currents and the Wiberg and Harris method for waves.*
MEAN DIAMETER OF THE SEDIMENT*;* SEDIMENT DIAMETERS	.01;.01;.01;.01;.01; .01;.01;.01;.01;.01	*Sets value of diameter for a particular size class [m]*
INITIAL FRACTION FOR PARTICULAR SIZE CLASS	1.;0.;0.;0.;0.; 0.;0.;0.;0.;0.	*Sets value of initial fraction for particular size class*
MPM COEFFICIENT	8.0	= α_{mpm}; Meyer-Peter and Müller Coefficient [-]
SHIELDS PARAMETERS	-	*Used to determine the critical bed shear stress value (non-cohesive sediments). For multi grain size, the shields parameter needs to be specified for each class. If only one value is specified, the shields parameter will be considered constant. The default option (no shields given in parameter file) is to calculate the shields parameter as a function of sand grain diameter (see logical CALAC).*
COEFFICIENT FUNCTION OF THE POROSITY	0.4	*The bed volume concentration CSF=(1-porosity) is used to calculate the bed evolution of non-cohesive sand transport.*
HIDING FACTOR FORMULA	0	*4 hiding factor formulas are implemented in SISYPHE* *0: const => need to give HIDING FACTOR FOR PARTICULAR SIZE CLASS* *1: Egiazaroff* *2: Ashida \& Michiue* *4: Karim, Holly \& Yang*
HIDING FACTOR FOR PARTICULAR SIZE CLASS	1.;1.;1.;1.;1.; 1.;1.;1.;1.;1	*Sets value of hiding factor for particular size class*

WATER VISCOSITY	1.0E-6	*Specifies the water kinematic viscosity [m/s²].*
FORMULA FOR DEVIATION	1	*1: Koch and Flokstra, 1981* *2: formula of Talmon et al., 1995*
PARAMETER FOR DEVIATION	0.85	*Parameter for the deviation caused by the slope according to the formula of Talmon et al., 1995. A high value will provoque a weak deviation.*
FORMULA FOR SLOPE EFFECT	1	*1 : formula of Koch et Flokstra, modification of bed load* *linked keyword : BETA* *2 : formula of Soulsby, modification critical shear stress,* *can only be used with a threshold fomula.* *linked keyword : FRICTION ANGLE OF THE SEDIMENT*
FRICTION ANGLE OF THE SEDIMENT	40	*Angle of repose of the sediment. Used in the Soulsby formula to take into account the influence of bed slope on critical shear stress. Use if* FORMULA FOR SLOPE EFFECT *=2*
BETA	1.3	*Specifies the value of the beta coefficient used in the Koch and Flokstra slope effect formulation*
SECONDARY CURRENTS	NO	*using the parametrization for secondary currents*
SECONDARY CURRENTS ALPHA COEFFICIENT	1	*Alpha coefficient of secondary current [-], Should be chosen between 0.75 (rough bottom) and 1 (smooth bottom)*

Appendix B: steering files TELEMAC-3D and SISYPHE

TELEMAC-3D: Scaldis 3D HD

here is the steering file of the TELEMAC-3D simulation

```
TITLE ='TELEMAC3D : 2050_REF_A0CN'

/-----------------------------------------------------------------------/
/                  INPUT-OUTPUT, FILES                                  /
/-----------------------------------------------------------------------/
FORTRAN FILE                    ='Scaldis_SIS_V7P2r1.f'
LIQUID BOUNDARIES FILE     ='Up_QN_2013_sedi3d.txt'
GEOMETRY FILE                   ='geo_v23_2013_Ref_QN_A0.slf'
BOUNDARY CONDITIONS FILE ='geo_v23_2013_REF_conlim.cli'
2D RESULT FILE                  ='r2D_2013REF_A0CN_SIS.slf'
3D RESULT FILE                  ='r3D_2013REF_A0CN_SIS.slf'
FORMATTED DATA FILE 2     ='Seaboundary_QN_2013_for2050grid_WLUV.txt'
CULVERTS DATA FILE          ='Culvert_File_2013.txt'
NUMBER OF CULVERTS        =35
OPTION FOR CULVERTS       =2
TYPE OF SOURCES             =2
MAXIMUM NUMBER OF SOURCES =150
/-----------------------------------------------------------------------/
/                RESTART FILE                                           /
/-----------------------------------------------------------------------/
PREVIOUS COMPUTATION FILE          ='HOTSTART_2013REF_A0CN'
PREVIOUS COMPUTATION FILE FORMAT = 'SERAFIND'
COMPUTATION CONTINUED              =YES
INITIAL TIME SET TO ZERO           =NO
SISYPHE STEERING FILE              ='SIS_QN_2013REF_A0CN.cas'
COUPLING WITH                      = 'SISYPHE'
COUPLING PERIOD FOR SISYPHE        = 1
/-----------------------------------------------------------------------/
/   INPUT-OUTPUT,TIME STEP, GRAPHICS AND LISTING    /
/-----------------------------------------------------------------------/
TIME STEP                          =4.0
NUMBER OF TIME STEPS               =324000   /15 days
PARALLEL PROCESSORS                =192
GRAPHIC PRINTOUT PERIOD            =450
LISTING PRINTOUT PERIOD            =150
VARIABLES FOR 2D GRAPHIC PRINTOUTS = 'U,V,S,H,B,TA*'
VARIABLES FOR 3D GRAPHIC PRINTOUTS = 'Z,U,V,W,TA*'
ORIGINAL DATE OF TIME              = 2013;07;31
ORIGINAL HOUR OF TIME              = 22;20;00
MASS-BALANCE                       =YES
INFORMATION ABOUT MASS-BALANCE FOR EACH LISTING PRINTOUT = YES
/-----------------------------------------------------------------------/
/                  FRICTION                                             /
/-----------------------------------------------------------------------/
FRICTION COEFFICIENT FOR THE BOTTOM     =0.02
LAW OF BOTTOM FRICTION                  =4  / Manning
```

```
LAW OF FRICTION ON LATERAL BOUNDARIES             =5  /=Nikuradse Law
FRICTION COEFFICIENT FOR LATERAL SOLID BOUNDARIES    =0.054848
/-------------------------------------------------------------------/
/              EQUATIONS, BOUNDARY CONDITIONS                       /
/-------------------------------------------------------------------/
VELOCITY PROFILES                          =1;1;1;1;1;1;1;1;1
PRESCRIBED FLOWRATES                        =23;34.7;11.1;15.92;34.6;8.3;10.38;35;0
PRESCRIBED ELEVATIONS                      =1;1;1;1;1;1;1;1;1
OPTION FOR LIQUID BOUNDARIES       =1;1;1;1;1;1;1;1;1
TREATMENT OF FLUXES AT THE BOUNDARIES =1;1;1;1;1;1;1;1;1
/-------------------------------------------------------------------/
/              EQUATIONS, INITIAL CONDITIONS                        /
/-------------------------------------------------------------------/
NUMBER OF HORIZONTAL LEVELS   = 5
MESH TRANSFORMATION          = 2 /sigma transformation default=1
INITIAL ELEVATION           =1
INITIAL CONDITIONS           ='CONSTANT ELEVATION'
/-------------------------------------------------------------------/
/                 NUMERICAL PARAMETERS                              /
/-------------------------------------------------------------------/
MATRIX STORAGE                             =3
TREATMENT OF NEGATIVE DEPTHS       =2
MASS-LUMPING FOR DEPTH                     =1
MASS-LUMPING FOR VELOCITIES          =1
MASS-LUMPING FOR DIFFUSION         =1
/-------------------------------------------------------------------/
/                        TURBULENCE                                 /
/-------------------------------------------------------------------/
VERTICAL TURBULENCE MODEL                                          =2
COEFFICIENT FOR VERTICAL DIFFUSION OF VELOCITIES     =1.E-2
MIXING LENGTH MODEL                                                =3
HORIZONTAL TURBULENCE MODEL                                        =4
COEFFICIENT FOR HORIZONTAL DIFFUSION OF VELOCITIES =1.E-2
PRECONDITIONING FOR DIFFUSION OF K-EPSILON             =2
ACCURACY FOR DIFFUSION OF VELOCITIES                       = 1.E-5
MAXIMUM NUMBER OF ITERATIONS FOR DIFFUSION OF VELOCITIES = 201
CORIOLIS                                                           =YES
CORIOLIS COEFFICIENT                                               =1.13522E-04
/-------------------------------------------------------------------/
/                      ADVECTION                                    /
/-------------------------------------------------------------------/
ADVECTION STEP                                          =YES
SCHEME FOR ADVECTION OF VELOCITIES           =1
SCHEME FOR ADVECTION OF DEPTH                =5
SCHEME FOR ADVECTION OF TRACERS             =13
MAXIMUM NUMBER OF ITERATIONS FOR ADVECTION SCHEMES = 200  /default 10 and only applied to schemes 13 and 14
NUMBER OF SUB ITERATIONS FOR NON LINEARITIES    =1
SOLVER FOR VERTICAL VELOCITY                        =7
/-------------------------------------------------------------------/
/                                  DIFFUSION                        /
/-------------------------------------------------------------------/
SCHEME FOR DIFFUSION OF VELOCITIES           =1  /default implicit (0 value cancels diffusion)
SCHEME FOR DIFFUSION OF TRACERS              =1
SCHEME FOR DIFFUSION OF K-EPSILON            =1
IMPLICITATION FOR DIFFUSION                         =1. /default
SOLVER FOR DIFFUSION OF VELOCITIES           =7 /default choice from 1-8
OPTION OF SOLVER FOR DIFFUSION OF VELOCITIES    =7
/-------------------------------------------------------------------/
/                  PROPAGATION                                      /
```

```
/-----------------------------------------------------------------------/
PROPAGATION STEP                                    =YES    /default
ACCURACY FOR PROPAGATION                            =1.E-5  /default E-6
MAXIMUM NUMBER OF ITERATIONS FOR PROPAGATION  =500   /default
SOLVER FOR PROPAGATION                              =7     /keuze uit 1-8
FREE SURFACE GRADIENT COMPATIBILITY                  =0.9   /only used with wave equation
IMPLICITATION FOR DEPTH                             =0.55   /default
IMPLICITATION FOR VELOCITIES                        =1.    /default (value < 0.5 makes unstable)
INITIAL GUESS FOR DEPTH                             =1     /default (choice 0,1 or 2) speeds up computation
OPTION OF SOLVER FOR PROPAGATION                     =7     /default and only used if solver=7 GMRES
/-----------------------------------------------------------------------/
/                                   WIND                                /
/-----------------------------------------------------------------------/
WIND                                    =NO
OPTION FOR WIND                         = 2
COEFFICIENT OF WIND INFLUENCE      =0.565E-6
/-----------------------------------------------------------------------/
/                   TRACERS                                             /
/-----------------------------------------------------------------------/
NUMBER OF TRACERS                               = 1
NAMES OF TRACERS                                = 'SALINITY       PSU           '
INITIAL VALUES OF TRACERS                        = 0
PRESCRIBED TRACERS VALUES                       = 0.1;0.1;0.1;0.1;0.1;0.1;0.1;0.1;0.1;0.1
/SOLVER FOR DIFFUSION OF TRACERS                =7
/OPTION OF SOLVER FOR DIFFUSION OF TRACERS      =7
DENSITY LAW                                     =2
COEFFICIENT FOR VERTICAL DIFFUSION OF TRACERS   =1.E-6
COEFFICIENT FOR HORIZONTAL DIFFUSION OF TRACERS =1.E-6
PRECONDITIONING FOR DIFFUSION OF TRACERS       =2
DAMPING FUNCTION                                =3
/-----------------------------------------------------------------------/
/                               TIDAL FLATS                             /
/-----------------------------------------------------------------------/
TREATMENT ON TIDAL FLATS FOR VELOCITIES        =0
TREATMENT ON TIDAL FLATS FOR TRACERS           =0
TIDAL FLATS                                     =YES
OPTION FOR THE TREATMENT OF TIDAL FLATS        =1
&FIN
```

SISYPHE: Scaldis Sand

here follows the steering file of SISYPHE

```
/-----------------------------------------------------------------------/
/      COMPUTER INFORMATIONS                                            /
/-----------------------------------------------------------------------/
STEERING FILE                   ='SIS_QN_2013REF_A0CN.cas'
GEOMETRY FILE                   ='geo_v23_2013_Ref_QN_A0.slf'
BOUNDARY CONDITIONS FILE='geo_v23_2013_REF_conlim.cli'
RESULTS FILE                    ='res_SIS_QN_2013REF_A0CN.slf'

PRESCRIBED SOLID DISCHARGES =0;0;0;0;0;0;0;0;0;0
ORIGINAL DATE OF TIME     = 2013;07;31
ORIGINAL HOUR OF TIME     = 22;20;00
/-----------------------------------------------------------------------/
/      GENERAL INFORMATIONS                                             /
```

```
/-----------------------------------------------------------------------/
VARIABLES FOR GRAPHIC PRINTOUTS  = B,M,N,P,TOB,E,MU
GRAPHIC PRINTOUT PERIOD          = 450
MASS-BALANCE                     =YES
TETA                             = 0.5
/-----------------------------------------------------------------------/
/          BED SEDIMENT TRANSPORT                                       /
/-----------------------------------------------------------------------/
BED LOAD                         = YES
BED-LOAD TRANSPORT FORMULA       =30          / 30=total load according to Engelund-Hansen formula
SEDIMENT DIAMETERS               =0.00015  / =150 µm
MORPHOLOGICAL FACTOR              = 1
```

Appendix C: list of net sand erosion – sedimentation rates of Upper Sea Scheldt

Table 3 – sedimentation/erosion for polygons in the Upper Sea Scheldt

polygon nr.	sedimentation/erosion [x10³ tons/year]
32	-46,66
33	41,02
34	-18,45
35	27,21
36	-10,14
37	-3,70
38	47,98
39	70,53
40	16,05
41	89,34
42	-73,58
43	-118,09
44	-10,74
45	88,98
46	-47,07
47	-13,89
48	-24,24
49	-1,58
50	15,76
51	-33,19
52	1,00
53	1,23
54	37,90
55	-26,64
56	26,49
57	-18,16
58	-30,98
59	24,07
60	-6,97
61	-2,79
62	4,52
63	0,10
64	-7,63
65	5,10
66	2,54
67	14,62
68	-16,73
69	-1,41
70	0,79
71	13,91
72	0,09
73	-17,63
Durme	7,13
Gentbrugge	0,0614

DEPARTMENT **MOBILITY & PUBLIC WORKS**
Flanders hydraulics Research

Berchemlei 115, 2140 Antwerp
T +32 (0)3 224 60 35
F +32 (0)3 224 60 36
waterbouwkundiglabo@vlaanderen.be
www.flandershydraulicsresearch.be